Journal of Medicinal Chemistry

Article

Synthesis of (E)-8-(3-chlorostyryl)caffeine analogs leading to 9-deazaxanthine derivatives as dual A2A antagonists /MAO-B inhibitors.

Silvia Rivara, Giovanni Piersanti, Francesca Bartoccini, Giuseppe Diamantini, Daniele Pala, Teresa Riccioni, Maria Antonietta Stasi, Walter Cabri, Franco Borsini, Marco Mor, Giorgio Tarzia, and Patrizia Minetti

J. Med. Chem., **Just Accepted Manuscript** • DOI: 10.1021/jm301686s • Publication Date (Web): 02 Jan 2013

Synthesis of (*E*)-8-(3-chlorostyryl)caffeine analogs leading to 9-deazaxanthine derivatives as dual A_{2A} antagonists /MAO-B inhibitors

Silvia Rivara,[a]* Giovanni Piersanti,[b]* Francesca Bartoccini,[b] Giuseppe Diamantini,[b] Daniele Pala,[a] Teresa Riccioni,[c] Maria Antonietta Stasi,[c] Walter Cabri,[c] Franco Borsini,[c] Marco Mor,[a] Giorgio Tarzia[b] *and* Patrizia Minetti*[c]

[a] *Dipartimento di Farmacia, Università degli Studi di Parma, Viale G.P. Usberti 27 A, I-43124 Parma, Italy.*

[b] *Department of Biomolecular Sciences, University of Urbino, Piazza Rinascimento 6, I-61029 Urbino (PU), Italy.*

[c] *Sigma-Tau Industrie Farmaceutiche Riunite S.p.A., Via Pontina Km 30,400, I-00040 Pomezia, Italy.*

Reference authors: Giovanni Piersanti, Silvia Rivara, Patrizia Minetti

Silvia Rivara
Dipartimento di Farmacia
Università degli Studi di Parma
Viale G.P. Usberti 27/A
I-43124 Parma (Italy)
Phone: +390521905061
Fax: +390521905006
E-mail: silvia.rivara@unipr.it

Giovanni Piersanti
Dipartimento di Scienze Biomolecolari
Università degli Studi di Urbino
Piazza Rinascimento 6
I-61029 Urbino (PU), Italy
Phone: +390722303313
Fax: +390722303320
E-mail: giovanni.piersanti@uniurb.it

Patrizia Minetti
Sigma-Tau Industrie Farmaceutiche Riunite S.p.A.
Via Pontina Km 30,400
I-00040 Pomezia, Italy.
Tel: +390691393906
Fax: +390691393638
E-mail. Patrizia.Minetti@sigma-tau.it

Abstract

A systematic modification of the caffeinyl core and substituents of the reference compound (*E*)-8-(3-chlorostyryl)caffeine led to the 9-deazaxanthine derivative (*E*)-6-(4-chlorostyryl)-1,3,5,-trimethyl-1*H*-pyrrolo[3,2-*d*]pyrimidine-2,4-(3*H*,5*H*)-dione (**17f**) which acts as a dual antagonist of human A_{2a}/MAO-B inhibitor ($K_i(A_{2A})$ = 260 nM; IC_{50}(MAO-B) = 200 nM; IC_{50}(MAO-A) = 10 μM) and dose dependently counteracts haloperidol-induced catalepsy in mice from 30 mg/kg by the oral route. The compound is the best balanced A_{2A} antagonist /MAO-B inhibitor reported to date and it could be considered as a new lead in the field of anti-Parkinson's agents. A number of analogs of **17f** were synthesized and qualitative SARs are discussed. Two analogs of **17f**, namely **18b** and **19a**, inhibit MAO-B with IC_{50} of 68 nM and 48 nM, respectively, being from five to seven folds more potent than the prototypical MAO-B inhibitor deprenyl (IC_{50} = 334 nM).

Introduction

The complexity of the interactions among the several neurotransmitters acting within the central nervous system (CNS) and the difficulty in obtaining acceptable therapeutic options for the treatment of diseases such as depression, Alzheimer's (AD) and Parkinson's (PD) diseases has led to a number of attempts to discover compounds acting simultaneously on more than one of the neurotransmitters known to play a role in these disorders, particularly when their respective receptors are localized in identical or vicinal areas of the brain or when synergic actions among them have been shown.[1] In the case of PD the development of selective antagonists of the A_{2A} adenosine receptor ($A_{2A}R$) initially led to the discovery of a number of promising agents, such as (*E*)-8-(3-chlorostyryl)caffeine (CSC)[2] istradefylline (KW6002),[3] KF-17837,[4] DMPX and DPMTX,[5] various derivative of 3,7-dimethylxanthines,[6] MSX-2 and its prodrugs,[7] SCH 58261,[8] ZM241385,[9] CGS 15943[10] and ST1535[11] (Figure 1). In particular, the therapeutic potential of KW6002 for the treatment of PD has been extensively investigated through a number of clinical trials, which showed that this compounds significantly improved motor impairment and reduced "off" time when co-administered with levodopa.[12] The therapeutic application of two irreversible inhibitors of monoamine oxidase B (MAO-B), (*R*)-deprenyl and rasagiline, for alleviating the symptoms of PD,[13] the age-related increase in the expression of MAO-B,[14] its cerebral distribution[15] and the dual activity of CSC as A_{2A} antagonist and MAO-B inhibitor[16] led to the proposal of jointly down-regulating A_{2a} and MAO-B as a novel approach for treating PD and to the design of several A_{2A}/MAO-B dual-acting agents.[17]

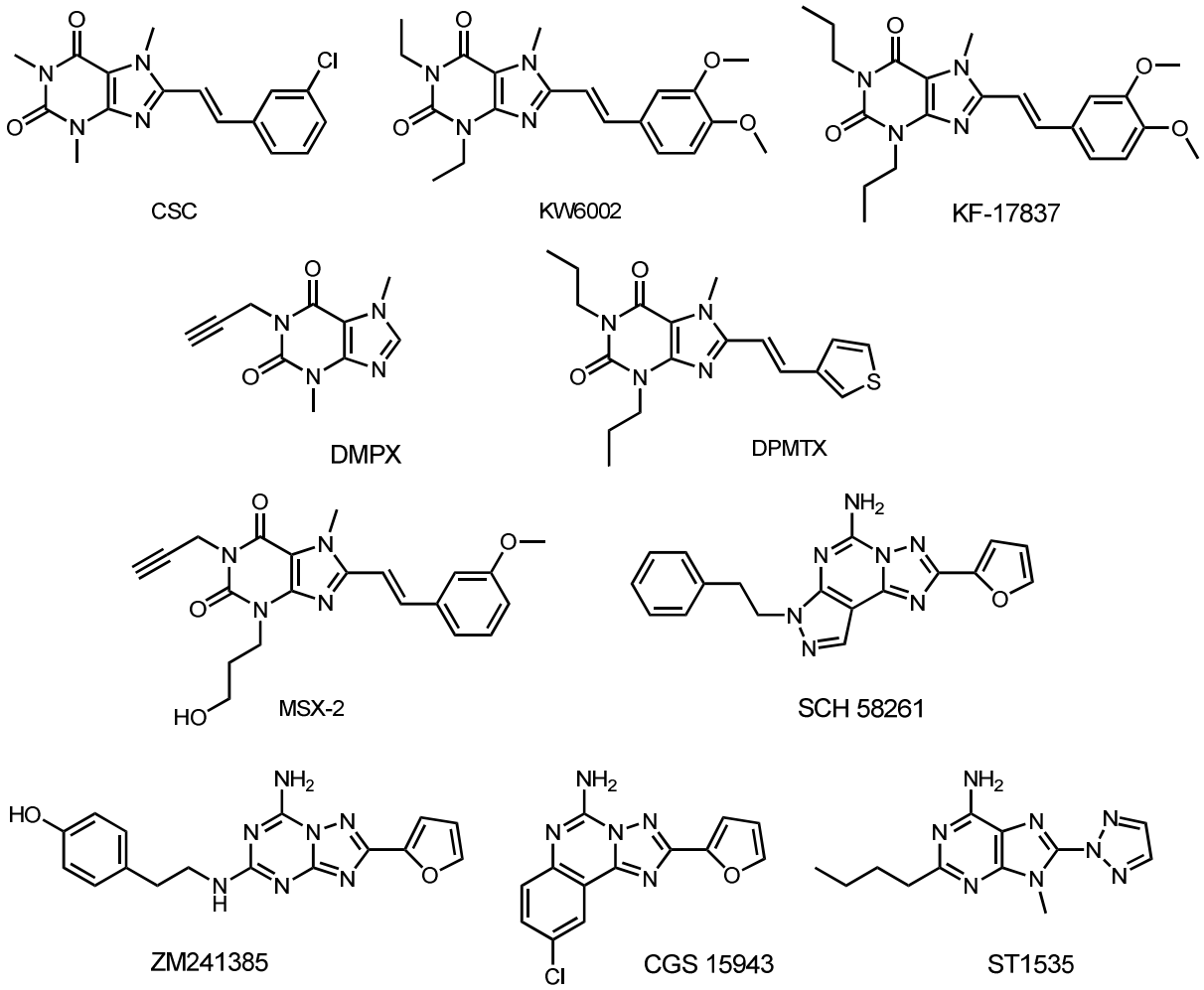

Figure 1. A_{2A} receptor antagonists.

Studies on dual-acting A_{2A} antagonists/MAO-B inhibitors are limited to compounds structurally related to caffeine and 8-styrylxanthine and the subject has been recently reviewed.[18] CSC is a reference dual-acting agent with good A_{2A} affinity (K_i = 36 nM on receptors expressed on rat brain striatal membranes)[6] and MAO-B inhibitory potency (K_i = 235 nM in tests performed on human liver mitochondria),[16b] effective *in vivo* in reversing the biochemical and behavioral modifications of 6-hydroxydopamine-lesioned rats.[19] We decided therefore to examine whether it could be possible to obtain new dual A_{2A} antagonists/MAO-B inhibitors with higher and more balanced potencies at the two targets. In order to select a suitable scaffold we run a preliminary exploratory modification of the caffeinyl core of CSC to obtain derivatives belonging to the different chemical

classes reported in Figure 2. In particular, we evaluated the role of the nitrogen, carbonyl group and imidazole ring in the purine system by preparing compounds **4a**,**b** and the pyrimidinedione derivative **6**. Bioisosteric replacement of the purine nitrogen atom in position 9 led to 9-deazaxanthines (**17a-y**, **18a-d**, **19a-d**, **20a,b**, **21-23**) and to their conformationally constrained tricyclic derivatives (**14a-c**). Preliminary screening of a few prototypes for their A_{2A}/MAO-B dual-activity allowed us to identify the 9-deazaxanthine as the most promising scaffold which was optimized by modifying the steric, electronic and lipophilic properties of the 8-substituent to give compound **17a-y**, **18a-d**, **19a-d**, **20a,b**, **21-23** (Figure 2, Schemes 1-8).

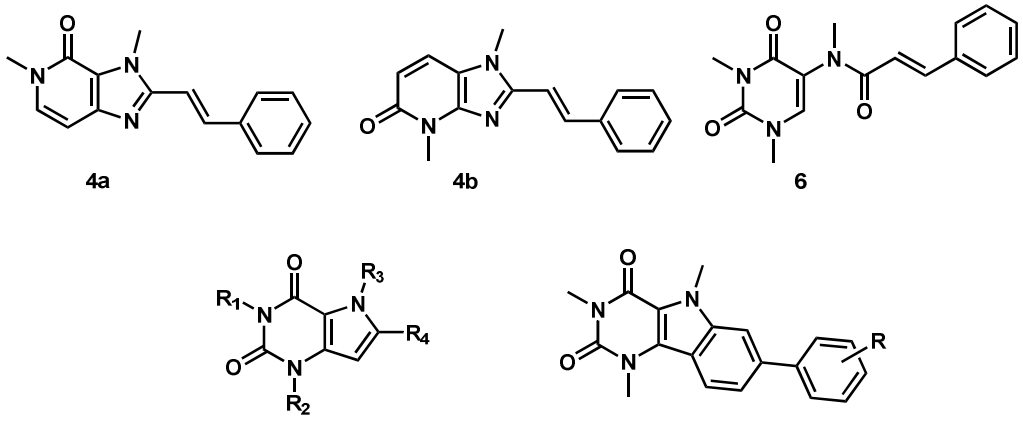

Figure 2. Chemical scaffolds of newly synthesized compounds.

Chemistry

The imidazopyridinones **4a,b** were obtained by direct condensation of **1a,b**[20] with *trans*-cinnamic acid or cinnamaldehyde to yield **2a,b** that were oxidized to **3a,b** with *m*-chloroperoxybenzoic acid (*m*-CPBA).[21] Rearrangement of **3a,b** with acetic anhydride[22] or trifluoroacetic anhydride[23] followed by *N*-alkylation with methyl iodide gave **4a,b** in satisfactory yields (Scheme 1).

Scheme 1. Synthesis of imidazopyridinone derivatives.[a]

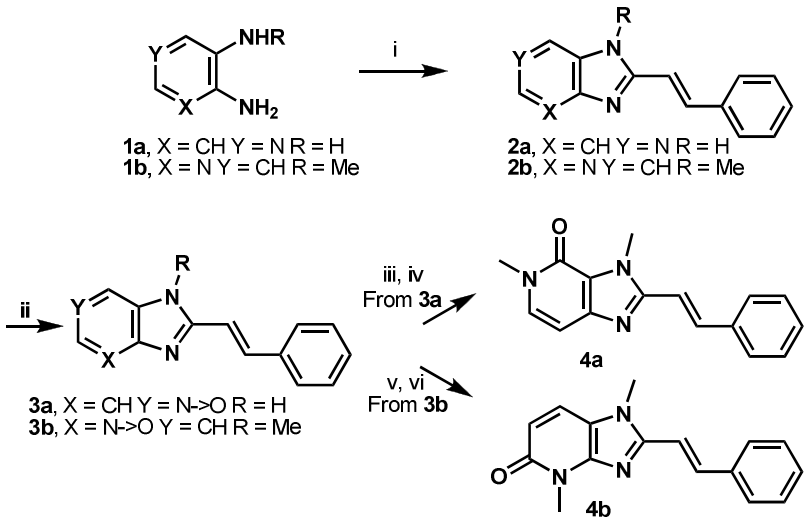

[a] Reagents and conditions: (i) For **2a**: (*E*)-PhCH=CHCO$_2$H, POCl$_3$, 140 °C, 5 h, 44%; For **2b**: MeOH, AcOH, (*E*)-PhCH=CHCHO, rt, 1 h, 40%; (ii) For **3a**: CH$_2$Cl$_2$, MeOH, *m*-CPBA, rt, 1 h, 68%; For **3b** CHCl$_3$, m-CPBA, rt, 30 min, 88%; (iii) (CH$_3$CO)$_2$O, 140 °C, 2 h, 56%. (iv) DMF, K$_2$CO$_3$, MeI, rt, 60 h, 28%; (v) DMF, (CF$_3$CO)$_2$O, rt, 16 h, 47%. (vi) NaOH 6 N, MeI, 50 °C, 12 h, 55%;

Amide coupling of the scarcely reactive secondary enamine **5**[24] with *trans*-cinnamic acid was obtained using 1-ethyl-3-(3-dimethylaminopropyl) carbodiimide (EDCI) as a coupling agent and afforded the desired amide (**6**) in modest yield. (Scheme 2).

Scheme 2. Synthesis of pyrimidines derivative **6**.[a]

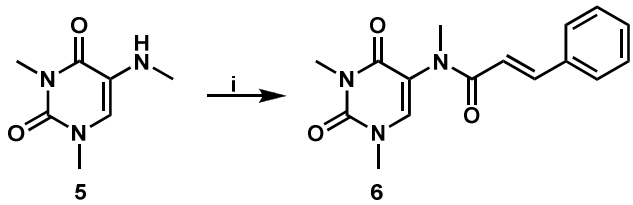

[a] Reagents and conditions: (i) MeOH, EDCI, PhCH=CHCO$_2$H, rt, 20 h, 37%.

1,3,5-Trimethyl-1*H*-pyrimido[5,4-*b*]indole-2,4(3*H*,5*H*)-dione derivatives **14a-c** were prepared as described in Scheme 3. Compound **14a** and **14c** were obtained respectively from the commercially

available **7a** and **9c**. Compound **14b** was obtained from **7b** which was synthesized by Suzuki reaction of 4-bromobenzaldehyde with 3-chlorophenylboronic acid.[25] Formation of ethyl 2-azidocinnamate (**8a,b**) by condensation of arylaldehyde (**7a,b**) with ethyl azidoacetate in the presence of sodium ethoxide at 0 °C and subsequently pyrolysis of **8a,b** in *p*-xylene a 150 °C gave the corresponding ethyl indole-2-carboxylate (**9a,b**). Reaction of indole derivatives **9a-c** and benzenediazonium chloride provided azo compounds **10a-c.** Reduction with tin and hydrochloric acid, followed by treatment with ethoxycarbonyl chloride, furnished carbamates **12a-c.** Cyclization with methylamine and N-methylation with methyl iodide provided **14a-c** (Scheme 3).

Scheme 3. Synthesis of 1,3,5-trimethyl-1*H*-pyrimido[5,4-*b*]indole-2,4(3*H*,5*H*)-dione derivatives.[a]

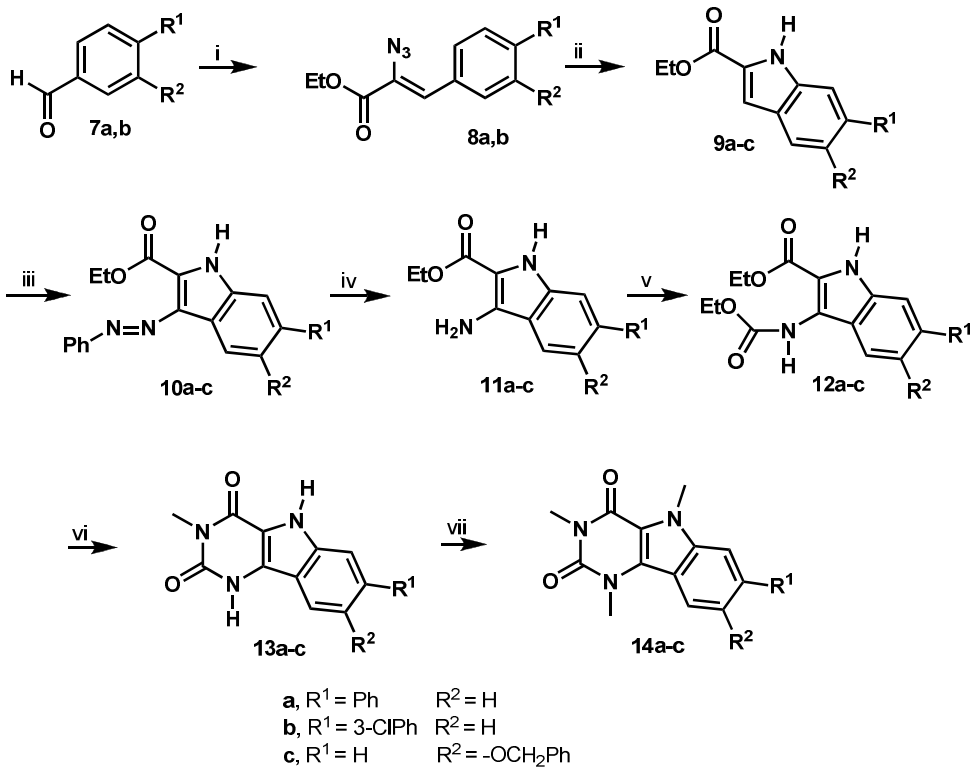

[a] Reagents and conditions: (i) EtOH, $N_3CH_2CO_2Et$, EtONa, 0 °C, 2h, 55-58%; (ii) *p*-xylene, 150 °C, 2 h, 78-98%; (iii) 1) $C_6H_5NH_2$, HCl 6 N, $NaNO_2$, 0 °C, 15'. 2) DMF, Na_2CO_3 2 N, 0 °C, 1 h, 30-80%; (iv) $(CH_3)_2CHOH$, conc. HCl, Sn, 85 °C, 2 h, 46-69%; (v) Xylene, ClCOOEt, 140 °C, 2 h, 40-83%; (vi) $(CH_3)_2CHOH$, CH_3NH_2 40% wt in H_2O, 85 °C, 24 h, 15-52%; (vii) DMF, NaH, MeI, rt, 24 h, 46-86%.

1,3,5-Trimethyl-6-styryl-*1H*-pyrrolo[3,2-*d*]pyrimidine-2,4(*3H,5H*)diones **17a-w** were obtained as described in Schemes 4 and 5. Compound **15a** was synthesized as previously reported[26] and the introduction of the styryl group was not without problems. Synthesis of styryl derivatives with electron-donating substituents was achieved by palladium cross-coupling reaction under standard reaction condition,[26] whereas the procedure failed in the case of styryl containing electron-withdrawing substituents. The vinylation of **15a** with vinyl boronate ester gave compound **16** which was used for Heck coupling with aryl bromides containing the electron withdrawing groups. Compounds **17a-n** were synthesized by path (ii), whereas compounds **17o-t** were prepared by path (iii) in Scheme 4.

Scheme 4. Synthesis of 8-styryl-9-deazaxanthine derivatives.[a]

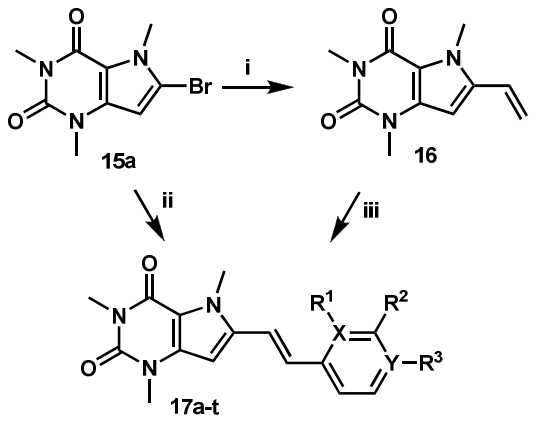

Compounds	X	Y	R^1	R^2	R^3	Compounds	X	Y	R^1	R^2	R^3
17a	C	C	H	Cl	H	**17k**	C	C	H	Cl	Cl
17b	C	C	H	H	H	**17l**	C	C	H	$-OCH_2O-$	
17c	C	C	H	OMe	H	**17m**	C	C	OMe	H	H
17d	C	C	H	CF_3	H	**17n**	N	C	H	NH_2	H
17e	C	C	H	H	F	**17o**	C	C	H	COMe	H
17f	C	C	H	H	Cl	**17p**	C	C	H	CN	H
17g	C	C	H	H	CF_3	**17q**	C	C	H	H	COMe
17h	C	C	H	H	OMe	**17r**	C	C	H	H	SO_2Me
17i	C	C	H	H	OnPr	**17s**	C	C	H	H	CN
17j	C	C	H	H	Br	**17t**	C	N	H	H	H

[a] Reagents and conditions: (i) DME, H_2O, CH_2=CHBpin, TEA, $PdCl_2(PPh_3)_2$, 80 °C, 16 h, 67%; (ii) DMF, KOAc, TBAB, molecular sieves, styrene derivatives, $Pd(OAc)_2$, 80 °C, 20 h, 20-86%; iii) DMF, aryl bromide, TEA, $P(o\text{-}tol)_3$, $Pd(OAc)_2$, 80 °C, 2 h, 30-84%.

Phenol derivatives **17u-w** were obtained by demethylation with BBr_3 of the corresponding methoxy derivatives **17c,h,m** (compound **17m** was not tested) (Scheme 5).

Scheme 5. Synthesis of hydroxystyryl derivatives.[a]

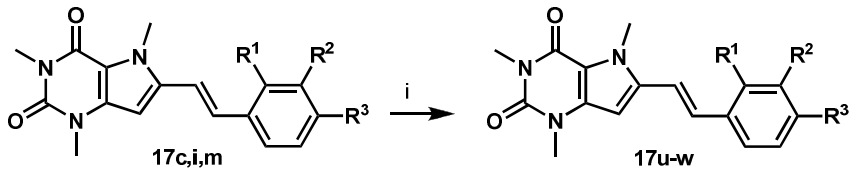

17c, $R^1 = R^3 = H$ $R^2 = OMe$
17h, $R^1 = R^2 = H$ $R^3 = OMe$
17m, $R^1 = OMe$ $R^2 = R^3 = H$

17u, $R^1 = R^3 = H$ $R^2 = OH$
17v, $R^1 = R^2 = H$ $R^3 = OH$
17w, $R^1 = OH$ $R^2 = R^3 = H$

[a] Reagents and conditions: (i) CH_2Cl_2, BBr_3 in CH_2Cl_2, 0 °C, 1 h, 27-90%.

Ethynyl derivatives **18a-c** were synthesized by Sonogashira reaction as previously reported[26] (Scheme 6).

Scheme 6. Synthesis of alkynyl derivatives.[a]

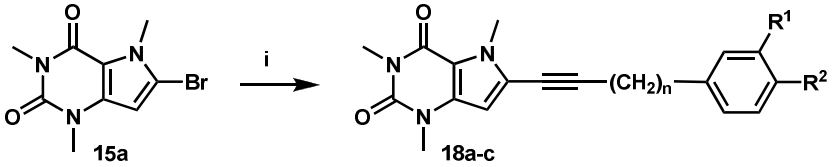

18a, n = 0 $R^1 = Cl$ $R^2 = H$
18b, n = 0 $R^1 = H$ $R^2 = Cl$
18c, n = 1 $R^1 = R^2 = H$

[a] Reagents and conditions: (i) Dioxane, TEA, CuI, $(PPh_3)_2PdCl_2$, alkynyl derivatives, 100 °C, 20 h, 54-62%.

The transition-metal-catalyzed formation of carbon-heteroatom bonds via cross-coupling reactions plays an important role in the preparation of numerous products of pharmaceutical interest,[27] allowing the introduction of various nitrogen- and oxygen-functions (amine, amide, urea, carbamate, alcohol, phenol, thiol) onto aromatic or heteroaromatic cycles. The bromo derivative

15a failed to give the desired N- or O-arylated products under variously modified reaction conditions (solvent, base, palladium and copper precursor, ancillary coligand), whereas the more reactive iodo derivative **15b**, prepared from **15a** by copper-catalyzed halogen exchange reaction using potassium iodide and *N,N'*-dimethylethylendiamine ligand[28] (Scheme 7), underwent copper or palladium-catalyzed coupling with different hetero-nucleophiles. Ether derivatives **19a-c** could be obtained in acceptable yield by copper-catalyzed reaction using 1,10-phenanthroline as a ligand at 110 °C for prolonged time. The same reaction condition did not work with phenols as substrates and the diarylethers **20a,b** were obtained by using ferric chloride as a catalyst in DMF in the presence of 2,2,6,6-tetramethyl-3,5-heptanedione and Cs_2CO_3 at 130 °C for 72 hours.[29] Copper (I) catalysts (bromide or iodide) allowed coupling of amides and triazoles[30] to give **21** and **22** in good yield. Similar reaction conditions permitted also a C-C bond formation by 2-C-H activation of the benzoxazole system to give compound **23** (Scheme 7).

Scheme 7. Synthesis of 8-functionalized deazaxanthine derivatives.[a]

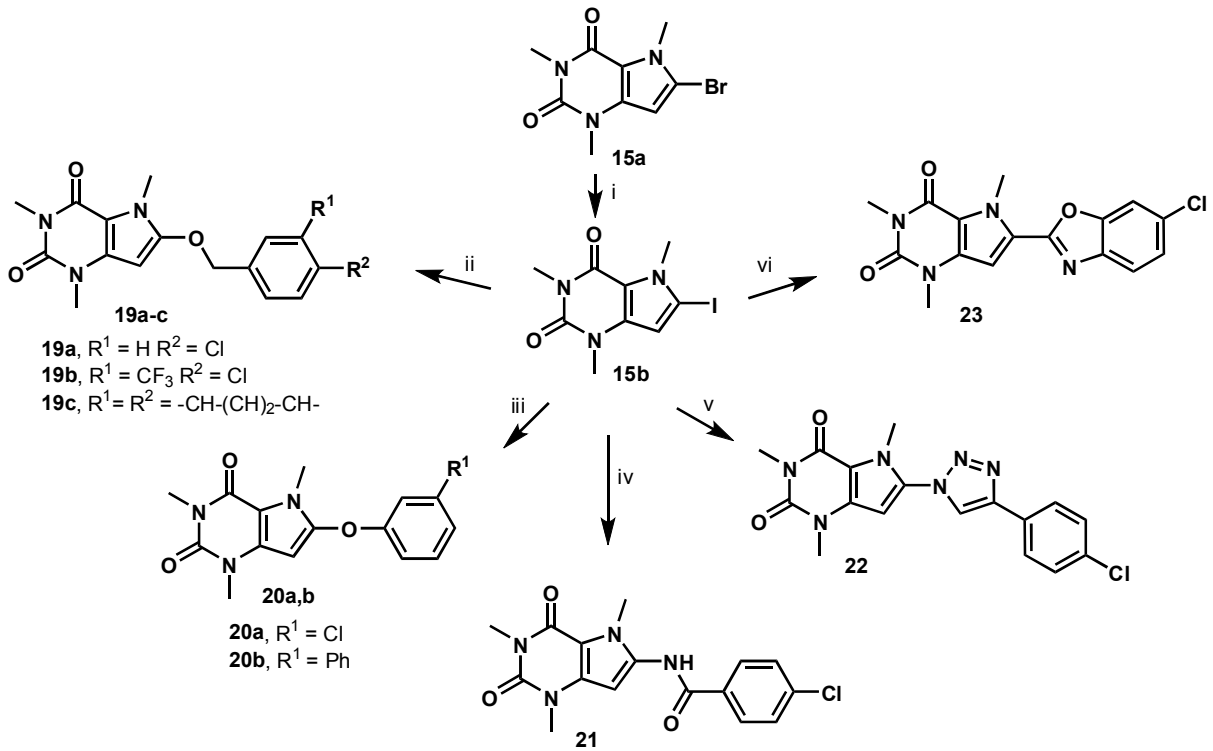

[a] Reagents and conditions: (i) CuI, KI, *N,N'*-dimethylethylendiamine, *n*-BuOH, 120 °C, 36 h, 72%;

(ii) Toluene, benzylalcohol derivatives, CuI, 1,10- phenanthroline, Cs_2CO_3, 100 °C, 5 h, 38-43%; (iii) DMF, phenol derivatives, $FeCl_3$, 2,2,6,6-tetramethyl-3,5-heptanedione, Cs_2CO_3,130 °C, 72 h, 37-43%; (iv) dioxane, K_2CO_3, CuI, *trans*-*N*,*N*'-dimethyl cyclohexan-1,2-diamine, 4-$ClC_6H_4CONH_2$, 100 °C, 20 h, 35%; (v) DMSO/H_2O 9:1, NaN_3, 4-$ClC_6H_4C{\equiv}CH$, $CuSO_4{\cdot}H_2O$, sodium ascorbate, L-Proline, 60 °C, 18 h, 39%; (vi) DMF, 6-chlorobenzo[*d*]oxazole, $Pd(OAc)_2$, P(t-Bu)$_3$, Cs_2CO_3, CuBr, 150 °C, 2 h, 39%.

The reaction conditions reported above were employed for the synthesis of different N-alkylated deazaxanthines (**17x,y**, **18d**, **19d**). In particular, compounds **17x,y** were synthesized by Heck coupling starting from **15c** and **15d,** respectively, compound **18d** was synthesized by Sonogashira coupling starting from **15d**, while compound **19d** was obtained by O-arylation of **15e** (Scheme 8).

Scheme 8. Synthesis of 8-functionalized deazaxanthine derivatives.[a]

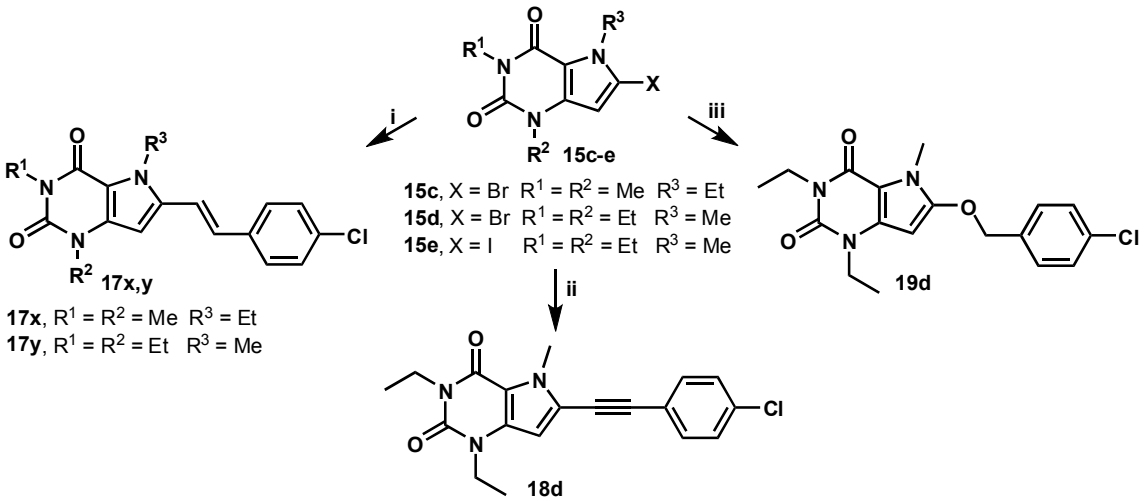

[a] Reagents and conditions: (i) DMF, KOAc, TBAB, molecular sieves, styrene derivatives, $Pd(OAc)_2$, 80 °C, 20 h, 43-45%; (ii) Dioxane, TEA, CuI, $(PPh_3)_2PdCl_2$, alkynyl derivatives, 100 °C, 20 h, 45%; (iii) Toluene, benzylalcohol derivatives, CuI, 1,10- phenanthroline, Cs_2CO_3, 100 °C, 5 h, 40%.

8-(p-Chlorostyryl)xanthine (**25**) was synthesized by a novel Pd/Cu-catalyzed dehydrogenative Heck coupling that allows direct alkenylation of caffeine (**24**) with 4-chlorostyrene (Scheme 9) which eliminates the need of preparing the heteroaryl halides.[31]

Scheme 9. Synthesis of 8-functionalized xanthine derivative.[a]

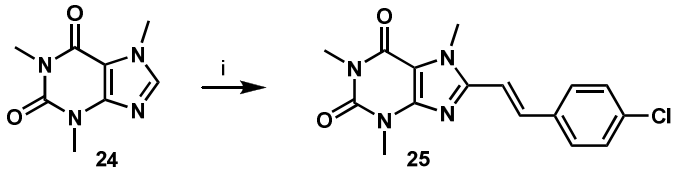

[a] Reagents and conditions: (i) 4-$ClC_6H_4CH{=}CH_2$, $Cu(OAc)_2$, $Pd(OAc)_2$, Ag_2CO_3, t-$BuCO_2H$, 90 °C, 72 h, 60%.

Results and discussion

The compounds were tested for their binding affinity for human A_{2A} (hA_{2A}) receptors and inhibitory potency on human MAO-B (hMAO-B) (Tables 1-3). Selectivity versus MAO-A was also evaluated for the compounds displaying MAO-B IC_{50} values lower than 1400 nM. Investigation on the structural determinants for the interaction with A_{2A} and MAO-B was initially focused on the pyrimidinedione moiety of the dechloro-CSC. Replacement by 1-methyl-2-pyridinone ring led to compound **4a**, which was inactive at both targets, and the same result was obtained with its regioisomer **4b** (Table 1). Deletion of the imidazole ring of the xanthine scaffold and insertion of an amide group on the pyrimidinedione ring (**6**) to maintain the coplanarity of the styryl substituent was also detrimental for the interaction with both targets. A more conservative modification, yielding the 9-deazaxanthine **17a** was tolerated by both targets, with only a limited decrease of potency (Table 1). The chlorine atom in position *meta* slightly decreased A_{2A} binding affinity, compared to the unsubstituted derivative **17b**, and had a negligible effect on MAO-B inhibitory potency. 8-Styryl-9-deazaxanthines have already been reported as A_2 receptor ligands,[32] but this is the first time that their MAO-B inhibitory potency is described. Crystal structures of the A_{2A} receptor in complex with caffeine and XAC (*N*-(2-aminoethyl)-2-[4-(2,3,6,7-tetrahydro-2,6-dioxo-1,3-dipropyl-1H-purin-8-yl)phenoxy]-acetamide) (where no water molecules were resolved)[33]

showed that the N9 of the xanthine nucleus does not directly interact with residues of the binding site (Figure 3A). On the other hand, superposition of the crystal structures of the A_{2A}-XAC complex with the recently solved A_{2A}-ZM241385 complex, where several water molecules are present,[34] showed that N9 of XAC is roughly superposed to the N4 of ZM241385, forming a hydrogen bond with a conserved water molecule belonging to a cluster located inside the binding site (Figure 3B). Lack of interaction with this cluster may explain the limited loss of binding affinity of the 9-deaza derivative **17a** compared to CSC.

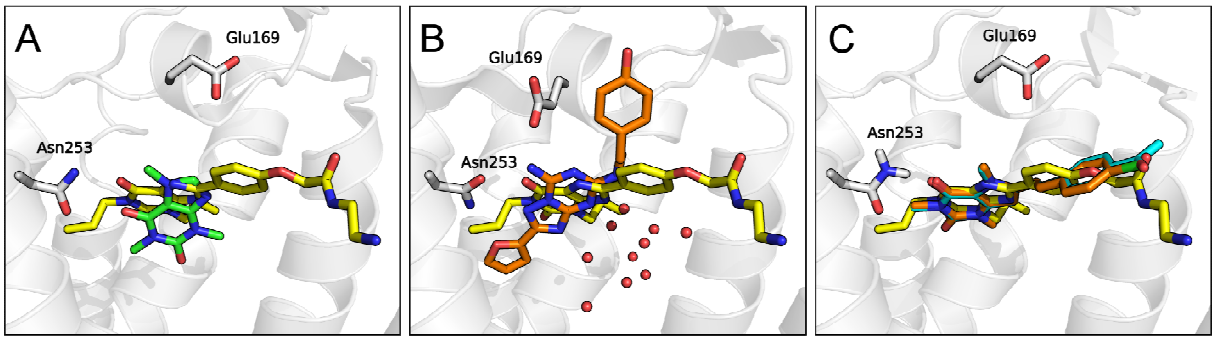

Figure 3. (A) Superposition of the crystal structures of A_{2A} receptor in complex with caffeine (green carbons, PDB code: 3RFM) and XAC (yellow carbons, PDB code: 3REY). (B) Superposition of the crystal structures of A_{2A} receptor in complex with ZM241385 (orange carbons, PDB code: 4EIY) and XAC (yellow carbons). Water molecules are represented with red spheres. (C) Best docking poses for compounds **17f** (orange carbons) and **17q** (cyan carbons) within the A_{2A} receptor structure built from 3REY. XAC molecule is depicted with yellow carbons.

No crystal structure is available for either xanthine or 9-deazaxanthine derivatives within the MAO-B catalytic site. We therefore docked CSC into the MAO-B crystal structure using Glide software [35] and Figure 4A depicts the best docking solution. CSC occupies both the substrate and the entrance cavities, with the xanthine moiety near the FAD cofactor and the 6-carbonyl group interacting with Tyr435 (not shown in Figure 4A). The purine core fits between Tyr398 and Leu171 on one side and Tyr435 and Gln206 on the other one. This accommodation is very similar to that described for some

8-benzyloxycaffeine analogs.[36] The 3-chlorostyryl protrudes into the entrance cavity in *s-cis* conformation, favored by the lower steric hindrance of N9 compared to the N7-methyl group. In this pose, the *m*-chlorine atom occupies the same region as the *m*-fluorine of safinamide and *m*-chlorine of some coumarin inhibitors (Figure 4B) in their crystallographic complexes.[37] The nitrogen atom in position 9 of CSC does not make polar interactions with the amino acids in the catalytic site. The best docking solution obtained for **17a** was strictly superimposable on that described for CSC (data not shown). To test the reliability of these poses, we constrained the *s-cis* geometry of the styryl group in the 9-deaza series into a pyrimido[4,5-*b*]indole nucleus (**14a-c**). This tricyclic ring could be docked within the MAO-B active site with the meta-chlorine of **14b** occupying the same position as that of 3-fluoro of safinamide (Figure 4A).

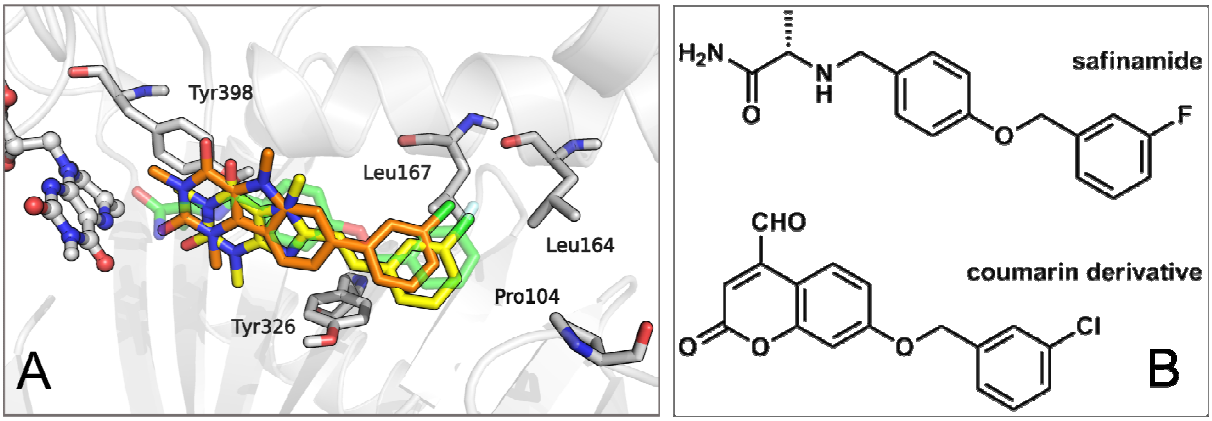

Figure 4. (A) Best docking poses for CSC (yellow carbons) and **14b** (orange carbons) within the MAO-B active site. The co-crystallized safinamide is depicted with green transparent carbons and the FAD cofactor in ball-and-sticks with white carbons. (B) Chemical structures of MAO-B inhibitors safinamide and coumarin derivative.

Consistently with what had been observed in the xanthine series,[17c] removal of the *m*-chlorine (**14a**) led to a decrease of inhibitory potency for MAO-B. Limited MAO-B inhibitory potency was also observed for compound **14c**, having a more flexible benzyloxy substituent in position 8.

Unfortunately, the tricyclic compounds were devoid of binding affinity for the A_{2A} receptor. For this reason we decided to abandon the exploration of pyrimido[4,5-*b*]indole scaffold and went back to the 9-deazaxanthine series. 8-Styryl-9-deazaxanthines did not strictly follow the same structure-activity relationships (SARs) as 8-styrylxanthines, lacking the positive effect of the *m*-chlorine group. This might be attributed to different equilibria between *s-cis* and *s-trans* conformations, and prompted us to further explore the SARs for this class of compounds. We thus focused on the role of substituents in position 1, 3, 7 and 8. Substituents with different size, shape, lipophilicity and electronic properties were introduced in *meta* or *para* position of the 8-styryl radical. *Meta* substituents did not lead to an increase of binding affinity for the A_{2A} receptor. Indeed, a chlorine (**17a**) or a methoxy group (**17c**) slightly reduced binding affinity, while trifluoromethyl (**17d**), hydroxyl (**17u**), acetyl (**17o**) or cyano (**17p**) substitution led to inactive compounds. Tests performed on rat A_2 receptors demonstrated that a *m*-chlorine doubled the binding affinity and that a *m*-methoxy and a *m*-trifluoromethyl were tolerated by the corresponding 8-styrylxanthine analogs, highlighting a different SAR profile.[2] *Meta*-substituted compounds carrying lipophilic groups had the highest MAO-B inhibitory potencies, with the best results obtained for the methoxy (**17c**) and the trifluoromethyl (**17d**) derivatives. Hydrophilic substituents were not tolerated (**17u**, **17p**). Compound **17c** was the best *meta*-substituted derivative, endowed with balanced potencies at the two targets, even if with limited MAO-B/MAO-A selectivity. On the 8-styrylxanthine series electron-withdrawing groups showed a more pronounced effect. Indeed, *m*-chlorine and *m*-trifluoromethyl increased inhibitory potencies about ten folds, compared to the four folds observed for the 8-styryl-9-deazaxanthine analogs.[17c]

A larger exploration was performed on the *para* position, but only the acetyl substituent (**17q**) led to a modest increase of A_{2A} binding affinity compared to the unsubstituted compound **17b**. Lipophilic substituents produced a limited decrease of binding affinity. Indeed, fluorine (**17e**), chlorine (**17f**), trifluoromethyl (**17g**) and methoxy (**17h**) groups were tolerated, as well as the longer n-propyloxy substituent (**17i**), while the bromine derivative **17j** completely lost A_{2A} binding affinity. Hydrophilic

methylsolfonyl (**17r**), cyano (**17s**) and hydroxyl (**17v**) groups were not tolerated. Lipophilic, electron-withdrawing groups, such as halogens (**17e**, **17f** and **17j**) and trifluoromethyl (**17g**), produced the greatest increase in MAO-B inhibitory potency. A *p*-chlorine and a *p*-trifluoromethyl substituent increased inhibitory potencies in the 8-styrylxanthine series as well, while fluorine had a negligible effect.[17c] Summarizing, different compounds with good potencies at both targets were obtained within the 8-(*para*-substituted-styryl)-9-deazaxanthines series, such as the acetyl (**17q**), fluorine (**17e**), trifluoromethyl (**17g**) and, in particular, the chlorine derivative **17f**. Compound **17f** (ST3564) is characterized by the best combination of A_{2A} binding affinity (K_i = 260 nM) and MAO-B inhibitory potency (IC_{50} = 200 nM) and it is selective versus MAO-A (IC_{50} = 10000 nM). It is more potent on MAO-B than CSC and the corresponding (*E*)-8-(4-chlorostyryl)caffeine (**25**), that we prepared and tested in our experimental conditions.

Other structural modifications were attempted on the 8-styryl-9-deazaxanthine scaffold. An *o*-hydroxyl group (**17w**) reduced the potency on both targets, as already observed for the same substituent in *meta* (**17u**) and *para* (**17v**) positions. The dichloro-derivative **17k** was the most potent MAO-B inhibitor in the 8-styryl-9-deazaxanthine series (IC_{50} = 133 nM), but it did not bind to A_{2A} receptors. A similar behavior was shown by compound **17l**, with a methylenedioxy portion bridging positions *meta* and *para*, which was tolerated at the MAO-B binding site only. The lack of A_{2A} binding affinity of **17l** represents another difference from the xanthine series. Indeed, 8-(3,4-dimethoxystyryl)caffeine had K_i = 18 nM and 1-propargyl-3,7-dimethyl-8-[3',4'-(methylenedioxy)styryl]xanthine had K_i = 35 nM on rat striatum A_{2A} receptors.[6] Replacement of the benzene ring in the styryl portion with a more hydrophilic and basic ring was detrimental for MAO-B inhibitory potency, as both the 4-pyridyl (**17t**) and 3-amino-2-pyridyl (**17n**) derivatives were inactive. Compound **17n** showed modest affinity for A_{2A} receptors, about five times lower than that of its benzene analog **17b**.

We prepared (*E*)-8-(4-chlorostyryl)caffeine (**25**) to compare *m*- and *p*-chlorine-substituted compounds. For both xanthine and 9-deazaxanthine series, *para* substitution resulted in higher hA_{2A} binding affinity and hMAO-B inhibitory potency than those observed for *meta* substitution.

As already stated, SARs for our 8-styryl-9-deazaxanthine derivatives are different from those reported on rat A_{2A} receptors for 8-styryl-xanthines, where *meta* substitution and *meta-para* disubstitution were favorable, contrary to what we observed on human receptor. On the other hand, *para* substitution with a chlorine atom gave higher hA_{2A} binding affinity in both series (**17f** and **25** for 8-styryl-9-deazaxanthine and 8-styryl-xanthine, respectively). To investigate if different binding modes could be supposed for the two series, we docked the most potent *para*-substituted 8-styryl-9-deazaxanthine derivatives **17f** and **17q** into the binding site of the A_{2A} receptor, co-crystallized with the xanthine derivative XAC. In their best docking poses the two compounds showed an accommodation inside the binding site very close to that of XAC, undertaking interactions with the same amino acids (Figure 3C), and 8-styryl-xanthines docked in the same pose as well (data not shown). Interestingly, the acetyl group of **17q** had its carbonyl superposed to the amide group of XAC. Therefore, no significant differences can be seen among the poses of the two classes, with the exception of the already cited possibility to undertake interactions with the cluster of water molecules within the binding site, and differences with SARs reported for 8-styryl-xanthines should be ascribed to different receptor origins.

The styryl substituent of (*E*)-8-styrylxanthines is known to undergo light-induced isomerization to the less potent *Z* isomer.[16b,38] We therefore investigated if it was possible to replace the 8-styryl group with substituents lacking the double bond, while maintaining the ability to interact with both targets. The benzyloxy group is typical of numerous MAO-B inhibitors, such as safinamide,[39] coumarin derivatives and also xanthine inhibitors.[37] We therefore prepared the 8-(*p*-chlorobenzyloxy)-9-deazacaffeine **19a**, as the *p*-chlorine derivative **17f** was the best one in the styryl series. Compound **19a** showed the highest MAO-B inhibitory potency (IC_{50} = 48 nM) in the whole series, about four folds higher than that of the styryl analog **17f** and with a good selectivity

versus MAO-A (Table 2). Unfortunately, it did not interact with the A_{2A} receptor. The presence of an additional *m*-trifluoromethyl group (**19b**) led to a ten fold decrease of MAO-B inhibitory potency with no effect on A_{2A} binding affinity, while an increase in the size of the substituent in the β-naphthylmethyloxy derivative **19c** led to a completely inactive compound. Shortening the 8-methyloxy linker to an oxygen atom, as in the *m*-chlorophenyloxy (**20a**) and *m*-biphenyloxy (**20b**) derivatives, was also detrimental for the ability to interact with both targets. On the other hand, replacement of the styryl double bond with a triple one led to the *m*-chlorophenyl- and *p*-chlorophenyl-ethynyl derivatives **18a** and **18b** having MAO-B inhibitory potencies higher than the corresponding styryl analogs. However, neither one showed affinity for the A_{2A} receptor. Differently, the 1-propargyl-3,7-dimethylxanthine carrying an 8-phenylethynyl substituent displayed K_i = 300 nM on A_{2A} receptors of rat striatum.[38] Insertion of a methylene spacer between the phenyl ring and the triple bond led to compound **18c** which was inactive at both targets. Replacement of the double bond with an amide group (**21**) or insertion of a 6-chlorobenzo[*d*]oxazol-2-yl substituent (**23**) in position 8 was not tolerated by either targets. When a 1,2,3-triazolyl ring replaced the ethylene linker (**22**) a good MAO-B inhibitory potency was maintained.

SARs for A_{2A} xanthine antagonists showed that longer alkyl substituents on the nitrogen atoms led to higher A_{2A} binding affinity than the corresponding methyl analogs.[2,38] Therefore we inserted ethyl groups in positions 1, 3, or 7 of the 9-deazaxanthine nucleus. Contrary to expectations, ethyl groups had a negative effect on potency, irrespective of the nature of the substituent in position 8. Inactive compounds at both targets were obtained with 8-(*p*-chlorostyryl) (**17y, 17x**), 8-(*p*-chlorophenylethynyl) (**18d**) and 8-(*p*-chlorobenzyloxy) (**19d**) substituents. This further confirms the different SAR profile observed for xanthine and 9-deazaxanthine derivatives.

Compound **17f**, having balanced A_{2A} /MAO-B activity, was tested against a panel of fifty-three receptors, ion channels and transporters.[40] At the concentration of 10 μM it produced 59% displacement of specific ligand at the A_1 receptor, 60% at the A_3 receptor and 91% at the A_{2A}

receptor. Compound **17f** appears therefore not selective for the A_{2A} subtype, having also affinity for the A_1 and A_3 subtypes. However, interaction with the A_1 receptor could be a positive element, due to the ability of A_1 antagonists to facilitate dopamine release and to counteract PD-related symptoms.[41] Compound **17f** did not significantly bind to other receptors or ion channels and transporters at 10 μM, with the exception of NK_2 and 5-HT_{2B} receptors and norepinephrine transporter, where it showed 75%, 72% and 57% displacement of specific ligands, respectively (Supplementary Table S2). General behavioral response and antagonism of haloperidol-induced catalepsy were evaluated in vivo for compound **17f**. In the Irwin test, compound **17f** induced striatal (biting and licking) and limbic (sniffing) stereotypes, after 90 minutes post treatment at the doses of 30 and 100 mg/kg. The dose of 100 mg/kg presented licking behavior after 240 minutes post treatment. No stereotypes were observed at the dose of 10 mg/kg. All the animals showed catalepsy before compound administration. Compound **17f** significantly antagonized haloperidol-induced catalepsy at doses of 30 and 100 mg/kg (Figure 5, $p<0.05$), while it was inactive at a dose of 10 mg/kg.

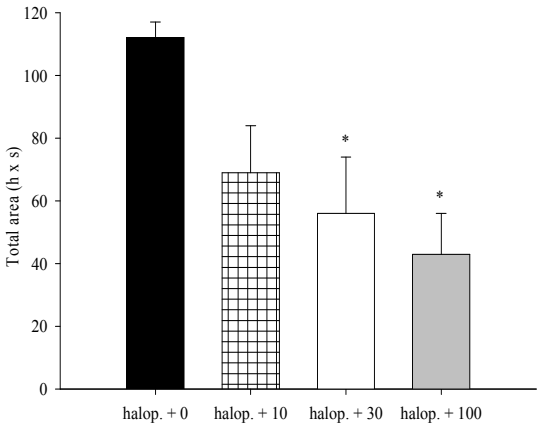

Figure 5. Dose-response curve of compound **17f** on haloperidol-induced catalepsy in mice (AUC). Columns represent mean + S.E.M. of 8 mice. Haloperidol (2 mg/kg) was administered i.p. 2.5 h before compound **17f**. AUC was calculated throughout three hours recording. One way Anova: $F_{3,28}=4.9$; $p<0.01$; Dunnett's test: * $p<0.05$ vs 0 mg/kg.

Conclusions

Structural modulation of CSC allowed us to obtain 9-deazaxanthine derivatives acting as A_{2A} antagonists/MAO-B inhibitors. Chemical exploration in position 8 of the 9-deazaxanthine scaffold provided the *p*-chlorostyryl derivative **17f** characterized by balanced potencies at the two targets, and by reversing haloperidol-induced catalepsy in mice. Replacement of the 8-styryl portion of CSC with either a benzyloxy (**19a**) or a phenylalkynyl (**18b**) substituent led to compounds with remarkable MAO-B inhibitory potencies, higher than those of CSC and deprenyl. Structural requirements for A_{2A} binding were stringent and could be met by 8-styryl derivatives only. SARs for 9-deazaxanthines were different from those reported for xanthines. The observed variance may be due either to differences in the structure of the two classes or in the biological tests that were used to characterize the compounds. Indeed, data for xanthines were mainly obtained from rat A_2/A_{2A} receptors and baboon or rat MAO-B, while our data come from human proteins.

Experimental Section

Chemistry

General methods. All reactions were run in air except when differently noted. Column chromatography purifications were performed in flash conditions using Merck 230-400 Mesh silica gel. Analytical thin layer chromatography (TLC) was carried out on Merck silica gel plates (silica gel 60 F254), that were visualized by exposure to ultraviolet light. ^{1}H NMR and ^{13}C NMR spectra were recorded on a Bruker Avance 200 spectrometer, using $CDCl_3$ or DMSO-d_6 as solvent. Chemical shifts (δ scale) are reported in parts per million (ppm) relative to the central peak of the solvent. Coupling constants (J values) are given in Hertz (Hz). EI-MS spectra (70 eV) were taken on a Fison Trio 1000, molecular ions (M+ or M-) are given. ESI-MS spectra were taken on a

Waters Micromass ZQ instrument, only molecular ions (M + 1 or M - 1) are given. IR spectra were obtained on a Nicolet Avatar 360 FT-IR spectrometer, absorbance are reported in cm^{-1}. Melting points were determined on a Buchi SMP-510 capillary melting point apparatus and are uncorrected. Elemental analyses were performed on a Carlo Erba analyzer and the results are within ± 0.4 of the theoretical values (C,H,N). Purity of tested compounds was greater than 95%.

General Procedure A for the Heck Coupling of 8-Halogen-9-deazaxanthine and styrene derivatives (17a-n,x,y). A flame-dried Schlenk tube was charged with potassium acetate (73 mg, 0.74 mmol), tetrabutylammonium bromide (119 mg, 0.37 mmol), powder 3Å molecular sieves (74 mg) and dry DMF (0.4 mL), the mixture was stirred for 15 minutes. The appropriate 6-Bromo-1,3,5-alkyl-1*H*-pyrrolo[3,2-*d*]pyrimidine-2,4(3*H*,5*H*)-dione (**15a,c,d**) (0.37 mmol) and the opportune styrene (0.74 mmol) was successively added and the suspension was stirred for another 15 minutes before addition of $Pd(OAc)_2$ (4 mg, 0.019 mmol). The mixture was stirred at 80 °C for 20 hours and then cooled at room temperature, diluted with CH_2Cl_2 (3 mL), filtered over Celite and washed with CH_2Cl_2 (3 x 10 mL). The solvent was evaporated under reduced pressure and the residue obtained was purified by flash chromatography (cyclohexane ethyl acetate 7:3).

For a representative example. (*E*)-6-(3-Chlorostyryl)-1,3,5-trimethyl-1*H*-pyrrolo[3,2-*d*]pyrimidine-2,4(3*H*,5*H*)-dione (17a): orange solid; (67 mg, 55%); **MS** (ESI): 330-332 $[M+H]^+$; **^{1}H NMR** ($CDCl_3$): δ 3.42 (s, 3H), 3.49 (s, 3H), 4.11 (s, 3H), 6.19 (s, 1H), 6.90 (d, 1H, *J* = 16.2 Hz), 7.08 (d, 1H, *J* = 16.2 Hz), 7.29-7.37 (m, 3H), 7.50 (s, 1H); **^{13}C NMR** ($CDCl_3$): δ 27.9, 31.7, 31.8, 90.9, 111.4, 116.1, 124.9, 126.3, 128.5, 130.1, 131.4, 134.9, 135.6, 138.1, 139.5, 151.5, 155.8; **FTIR** (nujol, cm^{-1}): 1647, 1685, 2854, 2924; **mp:** decomposition with color change starting from 200 °C (ethanol); Anal. ($C_{17}H_{16}ClN_3O_2$) C, H, N.

General Procedure B for the Heck Coupling of 8-vinyl-9-deazaxanthine and aryl bromide (17o-t). A flame-dried Schlenk tube was charged with 1,3,5-trimethyl-6-vinyl-1*H*-pyrrolo[3,2-

d]pyrimidine-2,4(3*H*,5*H*)-dione (**16**) (80 mg, 0.36 mmol), the opportune aryl bromide (0.73 mmol), TEA (0.24 mL, 1.69 mmol), P(o-tol)$_3$ (22 mg, 0.072 mmol), Pd(OAc)$_2$ (8 mg, 0.036 mmol) and dry DMF (3.6 mL). The mixture was stirred at 80 °C for 2 hours, under N_2 and then cooled at room temperature, diluted with CH_2Cl_2 (15 mL) and saturated aqueous sodium chloride solution (15mL). The phases were separated and the aqueous phase was extracted with further CH_2Cl_2 (15 mL). The combined organic phases were dried over anhydrous Na_2SO_4, the solvent was evaporated under reduced pressure and the residue obtained was purified by flash chromatography (gradient from cyclohexane/ ethyl acetate 7:3 to ethyl acetate/ methanol 9:1).

For a representative example. (*E*)-6-(4-Acetylstyryl)-1,3,5-trimethyl-1*H*-pyrrolo[3,2-*d*]pyrimidine-2,4(3*H*,5*H*)-dione (17q): yellow solid; (73 mg, 60%); MS (EI): 337 $(M)^+$; **^{1}H NMR** ($CDCl_3$): δ 2.62 (s, 3H), 3.42 (s, 3H), 3.49 (s, 3H), 4.12 (s, 3H), 6.23 (s, 1H), 7.14 (s, 2H), 7.58 (d, *J* = 8.5 Hz, 2H),7.98 (d, *J* = 8.5 Hz, 2H); **^{1}H NMR** (Acetone-d_6): δ 2.59 (s, 3H), 3.29 (s, 3H), 3.45 (s, 3H), 4.15 (s, 3H), 6.61 (s, 1H), 7.40 (d, *J* = 16.2 Hz, 1H), 7.54 (d, *J* = 16.2 Hz, 1H), 7.79 (d, *J* = 8.5 Hz, 2H), 8.01 (d, *J* = 8.5 Hz, 2H),; **^{13}C NMR** ($CDCl_3$): δ 26.5, 27.8, 31.6, 31.8, 91.2, 111.6, 117.2, 126.6, 129.0, 131.5, 135.6, 136.7, 139.4, 140.7, 151.5, 155.8, 197.1; **FTIR** (nujol, cm^{-1}): 1693, 1674, 1655; **mp:** decomposition with color change starting from 250 °C (ethanol); Anal. ($C_{19}H_{19}N_3O_3$) C, H, N.

Pharmacology

Inhibitory potency on Monoamine Oxidase

Monoamine oxidase (MAO) activity was evaluated by a commercial kit (MAO-Glo Assay, Promega). The kit provides a homogeneous luminescent method for measuring MAO activity and the effects on it of test compounds. The assay is performed by incubating the MAO enzyme with a luminogenic MAO substrate, which is a derivative of beetle luciferin ((4*S*)-4,5-dihydro-2-(6-hydroxybenzothiazolyl)-4-thiazolecarboxylic acid) converted by MAO to methyl ester luciferin.

After the MAO reaction has been performed, the "Luciferin Detection Reagent" is added to simultaneously stop the MAO reaction, convert the methyl ester derivative to luciferin and produce light. The amount of light produced is directly proportional to MAO activity. The experiments was performed in duplicate in 96-well plates at room temperature. In each well, the reaction mixture was composed of 12.5 μL of MAO substrate at its K_m values, corresponding to a final concentration of 40 μM for reaction with MAO-A and 4 μM for reaction with MAO-B, 12.5 μL of test compounds and 25 μL of either human MAO-A or MAO-B (Sigma) at a final concentration of 1 μg of protein/well. After one h of incubation, 50 μL/well of "Luciferin Detection Reagent" was added to each well and, after additional 20 min of incubation to generate and stabilize the luminescent signal, the plate was read at the luminometer (Wallac Victor). The net signal from reactions of substrate and MAO enzyme in the absence of inhibitors represents the positive control (total MAO activity), whereas the signal from reaction of substrate and inhibitors without MAO enzyme represents the negative control. Compounds were first examined at a fixed concentration of 10 and 1 μmol/L. Then, if active at this concentration, a concentration-response curve was performed. Results were expressed as percent of control values and, in the case of multiple concentrations, as IC_{50} (concentration causing a half maximal inhibition of control values). Four experiments were performed in duplicates.

A_{2A} receptor binding affinity

Membranes from human embryonic kidney (HEK) 293 cells, stably transfected with the human adenosine A_{2A} receptor gene, were used in the radioligand binding experiments. Competition binding experiments were performed incubating membranes (5-10 μg of protein/sample) with a single concentration of the A_{2A} antagonist [^{3}H]ZM241385 (Biotrend, Cologne, Germany) (2 nmol/L), in the presence of fixed concentrations of test compounds in 96-well filter plates (MultiScreen system, cat. MAFBN0B10, Millipore, Billerica, MA, USA) for one h at 4 °C in a total volume of 200 μL/well of appropriate buffer (50 mmol/L Tris-HCl, pH 7.4, 10 mmol/L $MgCl_2$).

Some compounds were retested at increasing concentrations ranging from 0.01 nmol/L to 10 µmol/L. Nonspecific binding was determined in the presence of 10 µmol/L cold ZM241385 (Tocris, Ellisville, MO, USA). At the end of incubation, bound and free radioligands were separated by filtering the 96-well filter plates using a Millipore filtration apparatus (MultiscreenHTS vacuum manifold). Filter plates were then washed several times with ice-cold buffer (50 mmol/L Tris-HCl, pH 7.4) and filter-bound radioactivity measured using a MicroBeta counter (PerkinElmer) after addition of 30 µL/well of OptiPhase SuperMix scintillation cocktail (PerkinElmer). Four experiments were performed in duplicates. IC_{50} values were determined by nonlinear fitting strategies with the program GraphPad Prism. The K_i values were calculated from the IC_{50} values in accordance with the Cheng-Prusoff equation.[42]

In-vivo experiments

All experiments were conducted in accordance with the guidelines for care and use of experimental animals of the European Communities Directive (86/609 EEC; 27.01.1992, No.116) and approved by the company veterinarian and the Italian Ministry of Health. Experiments were performed according to a randomized schedule. Compound **17f** (ST3564) was suspended in a solution containing 0.1% Tween 80 in 0.5 carboxymethylcellulose CMC (medium viscosity) (Sigma-Aldrich, Milan), that was used as vehicle. The drug was administered in a volume of 10 mL/kg in mice. Male CD-1 mice (Charles River, Calco, Italy), 5-6 wk old, were kept for 1 wk at 22 + 2, 22 + 2 °C, at 50 + 15 % relative humidity, with 15-20 air-volume/h changes, 12-h light/dark cycle (lights on at 07:00 hours). Animals were group-housed (n=10) in Makrolon R cages (42.5 cm x 26.6 cm x 16 high cm) with standard food pellets and water ad libitum.

Irwin test

The test was performed at 60 and 240 min after oral 10, 30 and 100 mg/kg administration of compound **17f**. Mortality was recorded during the 24 hr post-dose injection. General parameters (salivation, lacrimation, diarrhea, ptosis, tremors, convulsions, piloerection, Straub tail,

aggressiveness and stereotypes) and specific observations (loss of reflexes, catalepsy, motor activity, hot plate, body temperature and acute death) were recorded.

Catalepsy

Animals were gently placed by their forepaws on a small metal bar at a height of 4.5 cm. Catalepsy was induced by haloperidol (2 mg/kg) injected intraperitoneally 2.5 hours before oral administration compound **17f** (10, 30, 100 mg/kg) or vehicle. At time 0 minutes, successful induction of catalepsy in all animals was checked before compound administration, then, catalepsy was scored every 60 min for three hours. The catalepsy was measured as the time necessary for the animal to step down with at least one forepaw with a cut off time for each animal of 60 seconds; after this time the mouse was gently removed from the wire. Catalepsy was recorded using a video-camera and by an observer who was unaware of the treatment. Area under curve (AUC) throughout three hours was calculated and one-way Anova followed by Dunnett's test. Basal time was not included because this time-point was used only to check that catalepsy was successfully induced in all animals.

Molecular modeling

Molecular modeling was performed using the Schrodinger software suite. Receptor and ligand structures were prepared in Maestro 9.2[43] and refined using Macromodel 9.9.[44] Docking studies were carried out with Glide 5.7[35] using the SP scoring function. Default settings were used, unless stated otherwise.

Docking studies into MAO-B

The crystal structure of human MAO-B in complex with safinamide (PDB code: 2V5Z)[37] was selected for docking studies. After the correction of valences of the FAD cofactor and of the co-crystallized ligand, hydrogen atoms were added to the structure and protonation states for ionizable side chains were chosen to be consistent with physiological pH. The all-atoms receptor structure

was submitted to an energy minimization procedure using the MMFFs force field[45] to a convergence threshold of 0.05 kJ mol^{-1} $Å^{-1}$, holding all heavy atoms fixed. Starting structures of compound **14b** and CSC were minimized with the MMFFs force field to a convergence threshold of 0.05 kJ mol^{-1} $Å^{-1}$. Glide grids were centered on the co-crystallized safinamide, setting the enclosing box and bounding box dimensions to 30 Å and 10 Å, respectively. Twenty docking poses were collected for each ligand. The top-ranked poses according to the GlideScore value obtained for compound **14b** and CSC were merged into the MAO-B crystal structure and the resulting complexes were energy-minimized using the MMFFs force field to a convergence threshold of 5 kJ mol^{-1} $Å^{-1}$, keeping the protein backbone fixed.

Docking studies into A_{2A} receptor

The crystal structure of human A_{2A} receptor in complex with XAC (PDB: 3REY)[33] was retrieved from the Protein Data Bank and processed using the Protein Preparation Wizard. After the reconstruction of the missing Lys150-Gln157 sequence with Prime 3.0,[46] the protonation states for all ionizable side chains were assigned consistent with physiological pH. The overall hydrogen bonding network was optimized by adjusting the tautomerization states of histidine residues and by sampling the orientation of hydroxy and thiol groups, as well as the side chain amides of asparagine and glutamine residues. Protein C- and N-termini were capped with acetyl and methylamino groups, respectively. The all-atoms receptor structure was submitted to a restrained minimization procedure to the RMSD of 0.3 Å applying the OPLS2005 force field.[47] A loop refinement procedure was then performed with Prime[46] on the Pro149-Gly158 sequence to optimize the geometry of the newly-inserted residues. Ten different conformations were generated for the Pro149-Gly158 loop and the structure having the lowest energy was selected. Initial conformations of compounds **17f** and **17q** were energy-minimized applying a convergence threshold of 0.05 kJ mol^{-1} $Å^{-1}$ using the OPLS2005 force field.[47] Glide grids were centered on the co-crystallized XAC, setting the dimensions of enclosing and bounding boxes to 30 Å and 10 Å, respectively. Twenty docking poses were retained

for each ligand and subsequently ranked according to their GlideScore value. The top-ranked poses for compounds **17f** and **17q** were selected and are depicted in Figure 3C.

Supporting Information:

Experimental details and characterizations for compounds **2a,b**, **3a,b**, **4a,b**, **6**, **8a,b**, **9a,b**, **10a-c**, **11a-c**, **12a-c**, **13a-c**, **14a-c**, **17b-p,r-w**, **18a-d**, **19a-d**, **20a,b**, **21-23** and **25**; selectivity profile of compound **17f**. This material is available free of charge via the Internet at http://pubs.acs.org.

Table 1. A_{2A} adenosine receptor affinities (K_i) and MAO-B and MAO-A inhibitory potencies (IC_{50}) for the synthesized compounds.

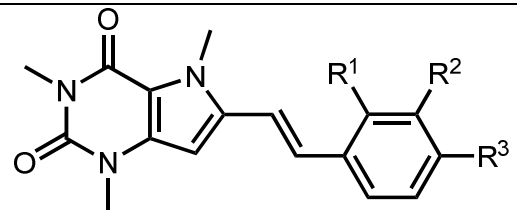

Compound		R^1	R^2	R^3	Ki hA_{2A} (nM)[a] (95% confidence interval)	IC_{50} hMAO-B (nM) (95% confidence interval)	IC_{50} hMAO-A (nM) (95% confidence interval)
Deprenyl						334.0 (260.7-427.9)	
Clorgyline							12.4 (11.6-13.2)
CSC					204.2 (90.2-462.5)	587.6 (260.7-1324.0)	
KW-6002					47.4 (15.7-143.3)	>10000	

4a	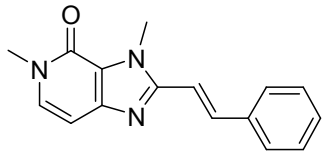				>10000	>10000	
4b	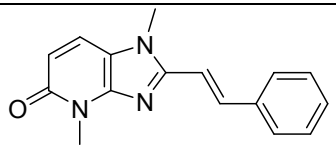				>10000	>10000	
6	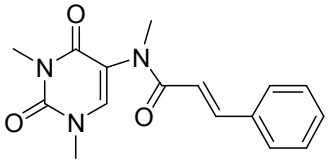				>1000	>10000	
14a	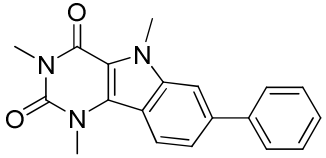				>10000	7630 (5610-10360)	
14b	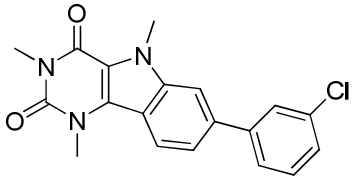				>1000	1390 (670-2870)	3110 (530-18400)

14c	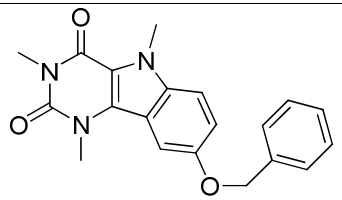				> 1000	5220 (2870-9480)	>10000
17a		H	Cl	H	430 (280-670)	1480 (600-3600)	
17b		H	H	H	170 (90-340)	1580 (800-3110)	
17c		H	OMe	H	390.5 (133.8-1140,0)	370.2 (279.3-490.6)	1237 (635.3-2407)
17d		H	CF_3	H	> 10000	480 (300-760)	5690 (500-66750)
17e		H	H	F	423.4 (283.6-632.1)	174.6 (93.4-326.5)	812.3 (515.1-1282.6)
17f (ST3564)		H	H	Cl	260 (160-420)	200 (50-900)	10000

17g		H	H	CF_3	530.6 (308.8-911.7)	431.5 (227.6-818.0)	>10000
17h		H	H	OMe	246.6 (118.3-514.1)	762.5 (580.2-1002.0)	>1000
17i		H	H	OnPr	306.9 (82.0-1148.0)	1368 (695.9-2689)	1300 (1056-1599)
17j		H	H	Br	>10000	266.7 (156.1-455.8)	1632 (840.0-3169)
17k		H	Cl	Cl	>10000	132.9 (33.5-527.5)	
17l		H	O-CH_2-O	>1000	467.3 (307.7-709.6)	>1000	
17n	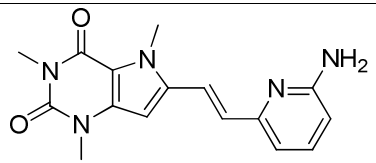				886.8 (31.3-25120)	>10000	
17o		H	COMe	H	>10000	>10000	

17p		H	CN	H	>10000	>10000	
17q		H	H	COMe	93.9 (34.9-252.6)	586.7 (347.8-989.9)	>10000
17r		H	H	SO_2Me	>1000	>1000	
17s		H	H	CN	>1000	543.3 (372.5-972.5)	>10000
17t	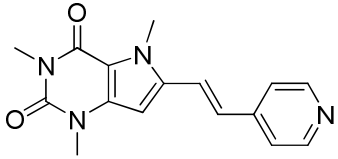				>10000	>10000	
17u		H	OH	H	>1000	>1000	
17v		H	H	OH	>10000	>10000	
17w		OH	H	H	1144.0 (441.0-2969.0)	>1000	
25	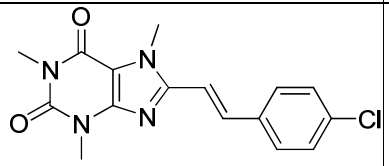				140.8 (67.4-294.2)	430.3 (319.4-579.8)	>10000

[a] K_i values were calculated from IC_{50} values, obtained from competition curves by the method of Cheng and Prusoff,[42] and are the mean of four determinations performed in duplicate.

Table 2. A_{2A} adenosine receptor affinities (K_i) and MAO-B and MAO-A inhibitory potencies (IC_{50}) for the synthesized compounds.

		Ki hA_{2A} (nM)[a] **(95% confidence interval)**	**IC_{50} hMAO-B (nM) (95% confidence interval)**	**IC_{50} hMAO-A (nM) (95% confidence interval)**
18a	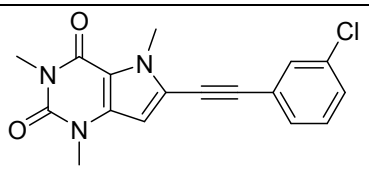	>10000	173.2 (122.8-244.3)	>10000
18b	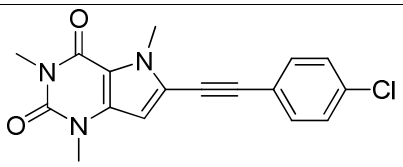	>10000	67.8 (23.4-196.2)	2022.0 (606.1-6749.0)
18c	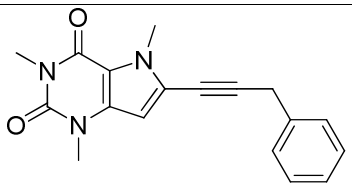	>10000	>1000	
19a	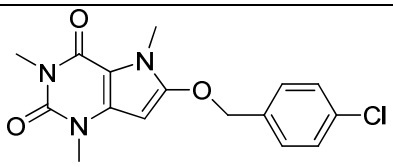	>10000	48.1 (21.1-109.9)	2870.0 (369.1-22320.0)
19b	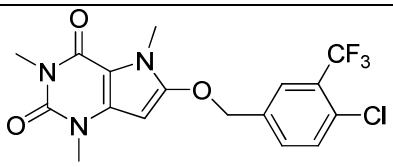	>10000	582.8 (461.7-735.6)	>10000
19c	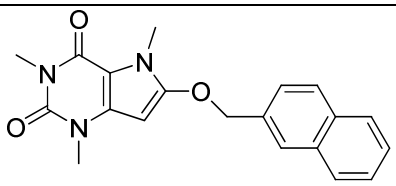	>10000	>1000	>10000

20a	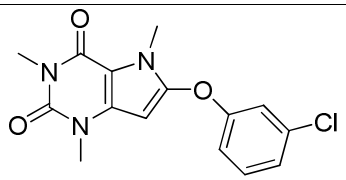	>10000	>10000	
20b	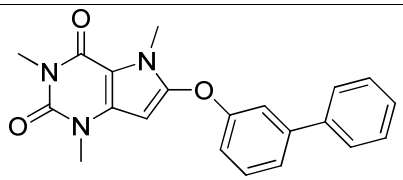	>10000	>10000	
21	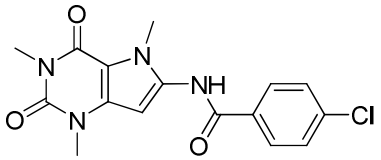	>10000	>10000	
22	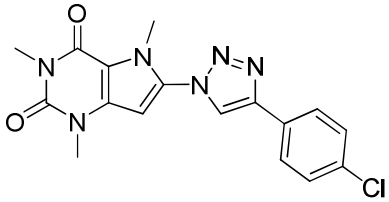	>10000	182.3 (117.2-283.7)	726.3 (342.1-1542.0)
23	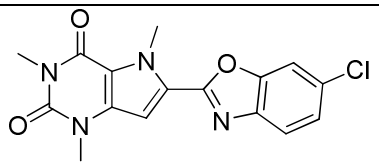	>1000	>1000	

[a] K_i values were calculated from IC_{50} values, obtained from competition curves by the method of Cheng and Prusoff,[42] and are the mean of four determinations performed in duplicate.

Table 3. A_{2A} adenosine receptor affinities (K_i) and MAO-B and MAO-A inhibitory potencies (IC_{50}) for the synthesized compounds.

		Ki hA_{2A} (nM)[a] (95% confidence interval)	**IC_{50} hMAO-B (nM) (95% confidence interval)**
17x	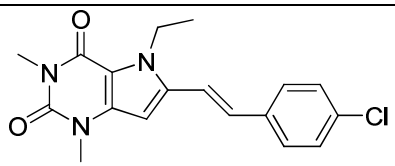	>10000	>1000
17y	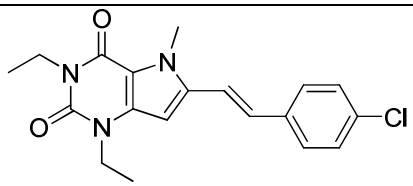	>10000	>1000
18d	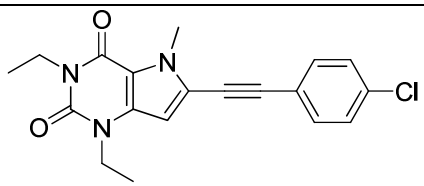	>10000	>1000
19d	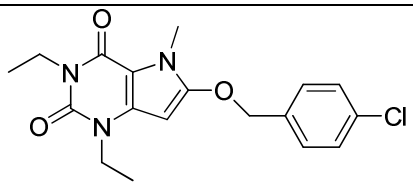	>10000	>1000

[a] K_i values were calculated from IC_{50} values, obtained from competition curves by the method of Cheng and Prusoff,[39] and are the mean of four determinations performed in duplicate.

Acknowledgements

We wish to thank Anna Maria Russo (Sigma Tau) for the excellent technical work. Authors from University of Urbino and Parma gratefully acknowledge financial support to the project from Sigma Tau.

Abbreviations used

AD, Alzheimer's disease; CNS, central nervous system; *m*-CPBA, *meta*-chloroperoxybenzoic acid; CSC, (*E*)-8-(3-chlorostyryl)caffeine; DME, 1,2-dimethoxyethane; DMF, dimethylformamide; EDCI, 1-ethyl-3-(3-dimethylaminopropyl)carbodiimide; MAO-B, monoamine oxidase B; PD, Parkinson's disease; SAR, structure-activity relationship; TBAB, tetrabutylammonium bromide; TEA, triethylamine.

Table of Contents Graphic

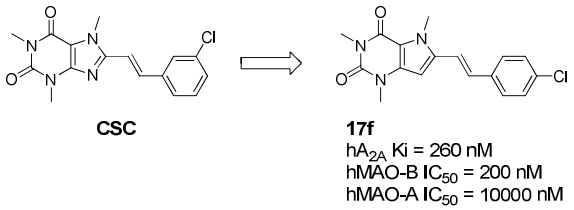

References

[1] (a) Rampa, A.; Belluti, F.; Gobbi, S.; Bisi, A. Hybrid-Based Multi-Target Ligands for the Treatment of Alzheimer's Disease. *Curr. Top. Med. Chem*. **2011**, *11*, 2716–2730. (b) Van der Schyf, C.J.; Geldenhuys, W.J. Multimodal Drugs and their Future for Alzheimer's and Parkinson's Disease. *Int. Rev. Neurobiol*. **2011**, *100*, 107–125. (c) Geldenhuys, W. J.; Youdim, M. B.; Carroll, R. T.; Van der Schyf, C. J. The Emergence of Designed Multiple Ligands for Neurodegenerative Disorders. *Prog. Neurobiol*. **2011**, *94*, 347–359.

[2] Jacobson, K. A.; Gallo-Rodriguez, C.; Melman, N.; Fischer, B.; Maillard, M.; van Bergen, A.; van Galen, P.J.; Karton Y. Structure-Activity Relationships of 8-Styrylxanthines as A2-Selective Adenosine Antagonists. *J. Med. Chem.* **1993**, *36*, 1333–1342.

[3] (a) Shimada, J.; Koike, N.; Nonaka, H.; Shiozaki, S.; Yanagawa, K.; Kanda, T.; Kobayashi, H.; Ichimura, M.; Nakamura, J.; Kase,H.; Suzuki, F. Adenosine A2A Antagonists with Potent Anti-Cataleptic Activity. *Bioorg. Med. Chem. Lett*. **1997**, *7*, 2349–2352. (b) Shiozaki, S.; Ichikawa, S.; Nakamura, J.; Kitamura, S.; Yamada, K.; Kuwana, Y. Actions of Adenosine A2A Receptor Antagonist KW 6002 on Drug-Induced Catalepsy and Hypokinesia Caused by Reserpine or MPTP. *Phychopharmacology* **1999**, *147*, 90–95. (c) Kase, H. The adenosine A2A receptor selective antagonist KW6002: Research toward a novel non-dopaminergic therapy for Parkinson's disease. *Neurology* **2003**, *61*, S97–S100.

[4] (a) Shimada, J.; Suzuki, F.; Nonaka, H.; Ishii, A.; Ichikawa, S. (E)-1,3-Dialkyl-7-methyl-8-(3,4,5 trimethoxystyryl)xanthines: Potent and Selective Adenosine A2 Antagonists. *J. Med. Chem*. **1992**, *35*, 2342–2345. (b) Nonaka, Y.; Shimada, J.; Nonaka, H.; Koike, N.; Aoki, N.; Kobayashi, H.; Kase, H.; Yamaguchi, K.; Suzuki, F. Photoisomerization of a Potent and Selective Adenosine A2 Antagonist, (E)-1,3-Dipropyl-8-(3,4-dimethoxystyryl)-7-methylxanthine. *J. Med. Chem*. **1993**, *36*, 3731–3733. (c) Suzuki, F.; Shimada, J.; Ishii, A.; Nonaka, H.; Kosaka, N.; Ichikawa, S. Xanthine

Derivatives. PCT Patent WO, 92/06976, 1992. (d) Correa, M., Wisniecki, A., Betz, A., Dobson, D. R., O'Neill, M. F., O'Neill, M. J., Salamone, J.D. The adenosine A2A antagonist KF17837 reverses the locomotor suppression and tremulous jaw movements induced by haloperidol in rats: Possible relevance to parkinsonism. *Behav. Brain Res*. **2004**, *148*, 47–54.

[5] Seale, T. W.; Abla, K. A.; Shamim, M. T.; Carney, J. M.; Daly, J. W. 3,7-Dimethyl-1-propargylxanthine: A potent and selective in vivo antagonist of adenosine analogs. *Life Sci.* **1988**, *43*, 1671–1684.

[6] Müller, C. E.; Geis, U.; Hipp, J.; Schobert, U.; Frobenius, W.; Pawłowski, M.; Suzuki, F.; Sandoval-Ramìrez, J. Synthesis and structure-activity relationships of 3,7-dimethyl-1-propargylxanthine derivatives, A2A-selective adenosine receptor antagonists. *J. Med. Chem.* **1997**, *40,* 4396–4405.

[7] (a) Sauer, R.; Maurinsh, J.; Reith, U.; Fülle, F.; Klotz, K.-N.; Müller, C. E. Watersoluble phosphate prodrugs of 1-propargyl-8-styrylxanthine derivatives, A2Aselective adenosine receptor antagonists. *J. Med. Chem*. **2000**, *43*, 440–448. (b) Hockemeyer, J.; Burbiel, J. C.; Müller, C. E. Multigram-scale syntheses, stability, and photoreactions of A2A adenosine receptor antagonists with 8-styrylxanthine structure: Potential drugs for Parkinson's disease. *J. Org. Chem*. **2004**, *69*, 3308–3318. (c) Vollmann, K.; Qurishi, R.; Hockemeyer, J.; Müller, C. E.. Synthesis and properties of a new water-soluble prodrug of the adenosine A2A receptor antagonist MSX-2. *Molecules* **2008**, *13*, 348–359. (d) Yang, M.; Soohoo, D.; Soelaiman, S.; Kalla, R.; Zablocki, J.; Chu, N., Leung, K.; Yao, L.; Diamond, I., Belardinelli, L.; Shryock, J. C. Characterization of the potency, selectivity, and pharmacokinetic profile for six adenosine A2A receptor antagonists. *Naunyn Schmiedebergs Arch. Pharmacol.* **2007**, *375*, 133–144.

[8] (a) Baraldi, P. G.; Manfredini, S.; Simoni, D.; Zappaterra, L.; Zocchi, C.; Dionisotti, S.; Ongini, E. Synthesis of New Pyrazolo-[4,3-*e*]1,2,4-triazolo[1,5-*c*]pyrimidine and 1,2,3-triazolo[4,5-*e*]1,2,4-triazolo[1,5-*c*]pyrimidine Displaying Potent and Selective Activity as A2A Adenosine Receptor

Antagonists. *Bioorg. Med.Chem. Lett.* **1994**, *4*, 2539–2544. (b) Zocchi, C.; Ongini, E.; Conti,A.; Monopoli, A.; Negretti, A.; Baraldi, P. G.; Dionisotti, S. The Non-Xanthine Heterocyclic Compound SCH 58261 is a New Potent and Selective A2A Adenosine Receptor Antagonist. *J. Pharmacol. Exp. Ther.* **1996**, *276*, 398–404. (c) Ongini, E. SCH58261: a Selective A2A Adenosine Receptor Antagonist. *Drug. Dev. Res.* **1997**, *42*, 63–70. (d) Baraldi, P. G.; Fruttarolo, F.;Tabrizi, M. A.; Preti, D.; Romagnoli, R.; El-Kashef, H.; Moorman, A.; Varani, K.; Gessi, S.; Merighi, S.; Borea, P. A. Design, Synthesis, and Biological Evaluation of C9- and C2-Substituted Pyrazolo[4,3-*e*]-1,2,4-triazolo[1,5-*c*]pyrimidines as New A2A and A3 Adenosine Receptors Antagonists. *J. Med. Chem*. **2003**, *46*, 1229–1241.

[9] (a) Caulkett, P. W. R.; Jones, G.; McPartlin, M.; Renshaw, N.D.; Stewart, S. K.; Wright, B. Adenine Isosteres with Bridgehead Nitrogen. Part 1. Two Independent Synthesis of the [1,2,4]-triazolo[1,5-*a*][1,3,5]triazine Ring System Leading to a Range of Substituents in the 2, 5 and 7 Positions. *J. Chem. Soc., Perkin Trans. 1* **1995**, *7*, 801–808. (b) Poucher, S. M.; Keddie, J. R.; Singh, P.; Stoggall, S. M.; Caulkett, P. W. R.; Jones, G.; Collis, M. G. The in *vitro* pharmacology of ZM 241385, a Potent, Non-Xanthine, A2A Selective Adenosine Receptor Antagonist. *Br. J. Pharmacol.* **1995**, *115*, 1096–1102.

[10] Francis, J. E.; Cash, W. D.; Psychoyos, S.; Ghai, G.; Wenk, P.; Friedmann, R. C.; Atkins, C.; Warren, V.; Furness, P.; Hyun, J. L.; Stone, G. A.; Desai, M.; Williams, M. Structure-Activity Profile of a Series of Novel Triazoloquinazoline Adenosine Antagonists. *J. Med. Chem.* **1988**, *31*, 1014–1020.

[11] (a) Minetti, P.; Tinti, M. O.; Carminati, P.; Castorina, M.; Di Cesare, M.-A.; Di Serio, S.; Gallo, G.; Ghirardi, O.; Giorgi, F.; Giorgi, L.; Piersanti, G.; Bartoccini, F.; Tarzia, G. 2-*n*-Butyl-9-methyl-8-[1,2,3]triazol-2-yl-9*H*-purin-6-ylamine and Analogues as A2A Adenosine Receptor Antagonists. Design, Synthesis, and Pharmacological Characterization. *J. Med. Chem.* **2005**, *48,* 6887–6896. (b) Bartoccini, F.; Cabri, W.; Celona, D.; Minetti, P.; Piersanti, G.; ,Tarzia, G. Direct B-Alkyl Suzuki

Miyaura Cross-Coupling of 2-Halopurines. Practical Synthesis of ST1535, a Potent Adenosine A2A Receptor Antagonist. *J. Org. Chem*. **2010**, *75*, 5398–5401. (c) Rose, S.; Jackson, M.J.; Smith L.A.; Stockwell, K.; Johnson, L.; Carminati, P.; Jenner, P. The novel adenosine A2a receptor antagonist ST1535 potentiates the effects of a threshold dose of L-DOPA in MPTP treated common marmosets. *Eur. J. Pharmacol.* **2006**, *546*, 82–87. (d) Tozzi, A.; Tscherter, A.; Belcastro , V.; Tantucci, M.; Costa, C.; Picconi, B.; Centonze, D.; Calabresi, P.; Borsini, F. Interaction of A2A adenosine and D2 dopamine receptors modulates corticostriatal glutamatergic transmission. *Neuropharmacology* **2007,** *53*, 783–789. (e) Tronci, E; Simola, N.; Borsini, F.; Schintu N.; Fraura, L.; Carminati, P.; Morelli, M. Characterization of the antiparkinsonian effects of the new adenosine A2A receptor antagonist ST1535: Acute and subchronic studies in rats. *Eur. J. Pharmacol.* **2000**, *566*, 94–102. (f) Rose, S.; Ramsay Croft, N.; Jenner, P.; The novel adenosine A2a antagonist ST1535 potentiates the effects of a threshold dose of L-dopa in unilaterally 6-OHDA-lesioned rats. *Brain Res.* **2007**, *1133*, 110–114. (g) Pinna, A.; Pontis, S.; Borsini, F.; Morelli, M. Adenosine A2A Receptor Antagonists Improve Deficits in Initiation of Movement and Sensory Motor Integration in the Unilateral 6-Hydroxydopamine Rat Model of Parkinson's Disease. *SYNAPSE* **2007**, *61*, 606–614. (h) Galluzzo, M.; Pintor, A.; Pèzzola, A.; Grieco, R.; Borsini,F.; Popoli, P. Behavioural and neurochemical characterization of the adenosine A2A receptor antagonist ST1535. *Eur. J. Pharmacol.* **2008**, *579*, 149–152. (i) Belcastro, V.; Tozzi, A.; Tantucci, M.; Costa, C.; Di Filippo, M.; Autuori, A.; Picconi, B.; Siliquini, S.; Luchetti, E.; Borsini, F.; Calabresi, P. A2A adenosine receptor antagonists protect the striatum against rotenone-induced neurotoxicity. *Exp. Neurol.* **2009**, *217*, 231–234. (j) Frau, L.; Borsini, F.; Wardas, J.; Khairnar, A.; Scjintu, N.; Morelli, M. Neuroprotective and Anti-inflammatory Effects of the Adenosine A2A Receptor Antagonist ST1535 in a MPTP Mouse Model of Parkinson's Disease. *SYNAPSE* **2011**, 65, 181–188.

[12] Park, A.; Stacy, M. Isradefillyne for the treatment of Parkinson's disease. *Expert Opin. Pharmacother*. **2012**, *13*, 111-114.

[13] (a) Gaines, K. D.; Hinson, V. K.; Adjuntive therapy in Parkinson's Disease: the Role of Rasagiline. *Neuropsychiatr. Dis. Treat.* **2012**, 8, 285–294. (b) Rascol, O.; Fitzer-Attas, C. J.; Hauser, R.; Jankovic, J.; Lang, A.; Langston, J. W.; Melamed, E.; Poewe, W.; Stocchi, F.; Tolosa, E.; Eyal, E.; Weiss, Y. M.; Olanow, C. W. A double-blind, delayed-start trial of rasagiline in Parkinson's disease (the ADAGIO study): pre-specified and post-hoc analyses of the need for additional therapies, changes in UPDRS scores, and non-motor outcomes. *Lancet/neurology* **2011**, *10*, 415–423. (c) Magyar, K.; Szende, B.; Jenei. V.; Tábi, T.; Pálfi, M.; Szökö, É. (R)-Deprenyl: Pharmacological Spectrum of its Activity. *Neurochem. Res.* **2010**, *35*, 1922–1932.

[14] (a) Nicotra, A.; Pierucci, F.; Parvez, H.; Santori, O. Monoamine oxidase expression during development and aging. *Neurotoxicology* **2004**, *25*, 155–165. (b) Fowler, J. S; Volkow, N. D.; Wang, G.-J.; Logan, J.; Pappas, N.; Shea, C.; MacGregor, R. Age-related increases in brain monoamine oxidase B in living healthy human subjects. *Neurobiol. Aging* **1997**, *18*, 431–435.

[15] Saura. J.; Beurl, Z.; Ulrich, J.; Mendelowitsch, A.; Chen, K.; Shih, J. C.; Malherbe, P.; Da Prada, M.; Richards, J. G. Molecular Neuroanathomy of Human Monoamine oxidases A and B Revealed by Quantitative Enzyme Radioautography and in situ Hybridization Histochemistry. *Neuroscience* **1996**, *70*, 755–774.

[16] (a) Chen, J. .; Steyn, S.; Staal, R.; Petzer, J. P.; Kui,X. van der Schyf, C. J.; Castagnoli, K.; Sonsalla, P. K.; Castagnoli, N. Jr.; Schwarzschild, M. A. 8-(3-Chlorostyryl)caffeine May Attenuate MPTP Neurotoxicity through Dual Actions of Monoamine Oxidase Inhibition and A2A Receptor Antagonism. *J. Biol. Chem* **2002**, 277, 36040–36044. (b) Petzer, J. P.; Steyn, S.; Castagnoli, K. P.; Chen, J.F.; Schwarzschild, M. A.; Van der Schyf, C. J.; Castagnoli, N. Inhibition of Monoamine Oxidase B by Selective Adenosine A2A Receptor Antagonists. *Bioorg. Med. Chem*. **2003**, *11*, 1299–1310. (c) van den Berg, D.; Zoellner, K. R.; Ogunrombi, M. O.; Malan, S. F.; Terre'Blanche,

G.; Castagnoli, N.; Bergh, Jr., J. J.; Petzer, J. P. Inhibition of Monoamine Oxidase B by Selected Benzimidazole and Caffeine Analogues.*Bioorg. Med. Chem.* **2007**, *15*, 3692-3702.

[17] (a) Kui, X.; Bastia, E.; Schwarzschild, M. Therapeutic potential of adenosine A2A receptor antagonists in Parkinson's disease. *Pharmacol. Ther.* **2005**, *105*, 267–310. (b) Schwarzschild, M. A.; L.; Agnati, Fuxe, K.; Chen, J.F.; Morelli, M. Targeting adenosine A2A receptors in Parkinson's disease. *Trends Neurosci*. **2006**, 29, 647–654. (c) Vlok, N.; Malan, S. F.; Castagnoli, N., Jr.; Bergh, J. J.; Petzer, J. P. Inhibition of monoamine oxidase B by analogues of the adenosine A2A receptor antagonist (E)-8-(3-chlorostyryl)caffeine (CSC). *Bioorg. Med. Chem.* **2006**, *14*, 3512–3521. (d) Pretorius, J.; Malan, S. F.; Castagnoli, N. Jr.; Bergh, J. J.; Petzer, J. P. Dual inhibition of monoamine oxidase B and antagonism of the adenosine A2A receptor by (E,E)-8-(4-phenylbutadien-1-yl)caffeine analogues. *Bioorg. Med. Chem.* **2008**, *16*, 8676–8684.

[18] (a) Petzer, J. P.; Castagnoli, N. Jr; Schwarzschild, M. A.; Chen, J.-F.; van der Schyf, C. J. Dual-Target–Directed Drugs that Block Monoamine Oxidase B and Adenosine A2A Receptors for Parkinson's Disease. *Neurotherapeuthics* **2009**, *6*, 141–151. (b) Armentero, M. T.; Pinna, A.; Ferré, S.; Lanciego, J. L.; Müller, C. E.; Franco, R. Past, present and future of A2A adenosine receptor antagonists in the therapy of Parkinson's disease. *Pharmacol. Ther.* **2011**, *132*, 280–299. (c) Pisani, L.; Catto, M.; Leonetti, F.; Nicolotti, O.; Stefanachi, A.; Campagna, F.; Carotti, A. Targeting Monoamine Oxidases with Multipotent Ligands: an Emerging Strategy in the Search of New Drugs Against Neurodegenerative Diseases. *Curr. Med. Chem.* **2011**, *18*, 4568–4587.

[19] Aguiar, L. M.; Macêdo, D. S.; Vasconcelos, S. M.; Oliveira, A. A.; de Sousa, F. C.; Viana, G. S. CSC, an adenosine A(2A) receptor antagonist and MAO B inhibitor, reverses behavior, monoamine neurotransmission, and amino acid alterations in the 6-OHDA-lesioned rats. *Brain Res*. **2008**, *1191*, 192–199.

[20] Collins, C. J.; Bupp, J. E.; Tanga, M. J. Synthesis of 2-amino-1-methyl-6-phenylimidazo[4,5-b]pyridine (PhIP), a heterocyclic food mutagen. *Arkivoc* **2002**, 90–96.

[21] Wang, T.-C.; Chen, Y.-L.; Lee, K.-H.; Tzeng, C.-C. Lewis Acid Catalyzed Reaction of Cinnamanilides: Competition of Intramolecular and Intermolecular Friedel-Crafts Reaction. *Synthesis* **1997**, 87–90.

[22] Crey-Desbiolles, C.; Lhomme, J.; Dumy, P.; Kotera, M. 3-Nitro-3-deaza-2‘-deoxyadenosine as a Versatile Photocleavable 2‘-Deoxyadenosine Mimic. *J. Am. Chem. Soc.* **2004**, *126*, 9532-9533.

[23] Konno, K.; Hashimoto, K.; Shirahama, H.; Matsumoto, T. Improved Procedures for Preparation of 2-Pyridones and 2-Hydroxymethylpyridines from Pyridine N-Oxides. *Heterocycles* **1986**, *24*, 2169–2172.

[24] Majumdar, K. C.; Mukhopadhyay C–C Bond Formation by Radical Cyclization: Synthesis of Pyrimidine-Annulated Heterocycles. *Synthesis* **2003**, *6*, 920–924.

[25] (a) Kataoka, N.; Shelby, Q.; Stambuli, J. P.; Hartwing, J. F. Air Stable, Sterically Hindered Ferrocenyl Dialkylphosphines for Palladium-Catalyzed C−C, C−N, and C−O Bond-Forming Cross-Couplings. *J. Org. Chem.* **2002**, *67*, 5553–5566; (b) Pawar, S. S.; Shingare, M. S.; Thore, S. N. A Novel Approach for Ligand Promoted Palladium (II)-Catalyzed Suzuki Coupling of Aryl Iodides and Bromides with Arylboronic Acid in Aqueous Media. *Lett. Org. Chem.* **2007**, *4*, 486–490.

[26] Bartoccini, F.; Piersanti, G.; Mor, M.; Tarzia, G.; Minetti, P.; Cabri W. Divergent Synthesis of Novel 9-Deazaxanthine Derivatives via Late-Stage Cross-Coupling Reactions. *Org. Biomol. Chem.*, **2012**, *10*, 8860–8867.

[27] (a) Torborg, C.; Beller, M. Recent Applications of Palladium-Catalyzed Coupling Reactions in the Pharmaceutical, Agrochemical, and Fine Chemical Industries. *Adv. Synth. Catal.* **2009**, *351*, 3027–3043. (b) Surry, D. S.; Buchwald, S. L. Biaryl Phosphane Ligands in Palladium-Catalyzed Amination. *Angew. Chem., Int. Ed.* **2008,** *47*, 6338–6361. (c) Hartwig, J. F. Evolution of a Fourth Generation Catalyst for the Amination and Thioetherification of Aryl Halides. *Acc. Chem. Res.* **2008**, *41*, 1534–1544.

[28] Klapars, A.; Buchwald, S. L. Copper-Catalyzed Halogen Exchange in Aryl Halides: An Aromatic Finkelstein Reaction. *J. Am. Chem. Soc.* **2002**, *124*, 14844–14845; b) Humphreys, J. L.; Lowes, D. J.; Wesson, K. A.; Whitehead, R. C. Arene *cis*-dihydrodiols—useful precursors for the preparation of antimetabolites of the shikimic acid pathway: application to the synthesis of 6,6-difluoroshikimic acid and (6*S*)-6-fluoroshikimic acid. *Tetrahedron* **2006**, *62*, 5099–5108.

[29] (a) Bistri, O.; Correa, A.; Bolm C. Iron-Catalyzed C-O Cross-Couplings of Phenols with Aryl Iodides. *Angew. Chem. Int. Ed.* **2008**, *47*, 586–588; (b) Xia, N.; Taillefer, M. Copper- or Iron-Catalyzed Arylation of Phenols from respectively Aryl Chlorides and Aryl Iodides. *Chem. Eur. J.* **2008**, *14*, 6037–6039; (c) Buchwald, S. L.; Bolm, C. Copper-Catalyzed Cross-Couplings with Part-per-Million Catalyst Loadings. *Angew. Chem. Int. Ed.* **2009**, *48*, 5691-5693; d) Buchwald, S. L.; Bolm, C. On the Role of Metal Contaminants in Catalyses with $FeCl_3$. *Angew. Chem. Int. Ed.* **2009**, *48*, 5586–5587.

[30] Andersen, J.; Bolvig, S.; Liang, X. Efficient One-Pot Synthesis of 1-Aryl 1,2,3-Triazoles from Aryl Halides and Terminal Alkynes in the Presence of Sodium Azide. *Synlett.* **2005**, 2941-2947.

[31] (a) Donghee, K.; Sungwoo, H. Palladium(II)-Catalyzed Direct Intermolecular Alkenylation of Chromones. *Org. Lett.*, **2011**, *13*, 4466–4469. (b) During the preparation of our manuscript, was reported a slightly different Dehydrogenative Heck coupling for the preparation of alkenylated xanthine, see Huang, Y.; Song, F.; Wang, Z.; Xi, P.; Wu, N.; Wang, Z.; Lan J.; You, J. Dehydrogenative Heck coupling of biologically relevant N-heteroarenes with alkenes: discovery of fluorescent core frameworks. *Chem. Commun.* **2012**, *48*, 2864–2866.

[32] Grahner, B.; Winiwarter, S.; Lanzner W.; Müller, C. E. Synthesis and Structure-activity relationships of deazaxanthines: analogs of potent A1- and A2-adenosine receptor antagonists. *J. Med. Chem.* **1994**, *37*, 1526–1534.

[33] Doré, A. S.; Robertson, N.; Errey, J. C.; Ng, I.; Hollenstein, K.; Tehan, B.; Hurrell, E.; Bennett, K.; Congreve, M.; Magnani, F.; Tate, C. G.; Weir, M.; Marshall, F. H. Structure of the adenosine

A(2A) receptor in complex with ZM241385 and the xanthines XAC and caffeine. *Structure* **2011**, *19*, 1283–1293.

[34] Liu, W.; Chun, E.; Thompson, A. A.; Chubukov, P.; Xu, F.; Katritch, V.; Han, G. W.; Roth, C. B.; Heitman, L. H.; IJzerman, A. P.; Cherezov, V.; Stevens, R. C. Structural basis for allosteric regulation of GPCRs by sodium ions. *Science* **2012**, *337*, 232–236.

[35] Glide, version 5.7, Schrödinger, LLC, New York, NY, 2011.

[36] Strydom, B.; Malan, S. F.; Castagnoli, N. Jr.; Bergh, J. J.; Petzer, J. P. Inhibition of monoamine oxidase by 8-benzyloxycaffeine analogues. *Bioorg. Med. Chem*. **2010**, *18*, 1018–1028.

[37] Binda, C.; Wang, J.; Pisani, L.; Caccia, C.; Carotti, A.; Salvati, P.; Edmondson, D. E.; Mattevi, A. Structures of human monoamine oxidase B complexes with selective noncovalent inhibitors: safinamide and coumarin analogs. *J. Med. Chem.* **2007**, *50*, 5848–5852.

[38] Müller, C. E.; Schobert, U.; Hipp, J., Geis, U.; Frobenius, W.; Pawlowski M. Configurationally stable analogs of styrylxanthines as A2A adenosine receptor antagonists. *Eur. J. Med. Chem*. **1997**, *32*, 709–719.

[39] Caccia, C.; Maj R.; Calabresi, M.; Maestroni, S.; Faravelli, L.; Curatolo, L.; Salvati, P.; Fariello, R. G. Safinamide: from molecular targets to a new anti-Parkinson drug. *Neurology* **2006**, *67*, S18-S23.

[40] Tests performed by Cerep. For experimental details, see http://www.cerep.fr/cerep/users/pages/catalog/assay/catalog.asp

[41] Trevitt, J.; Kawa, K.; Jalali, A,.; Larsen. C. Differential effects of adenosine antagonists in two models of parkinsonian tremor. *Pharmacol. Biochem. Behav.* **2009**, *94*, 24-9.

[42] Cheng, Y. C.; Prusoff, W. H. Deoxyribonucleotide Metabolism in Herpes Simplex Virus Infected HeLa Cells. *Biochem. Pharmacol.* **1973**, *22*, 3099–3108.

[43] Maestro, version 9.2, Schrödinger, LLC, New York, NY, 2011.

[44] MacroModel, version 9.9, Schrödinger, LLC, New York, NY, 2011.

[45] Halgren T.A. MMFF VII. Characterization of MMFF94, MMFF94s, and other widely available force fields for conformational energies and for intermolecular-interaction energies and geometries. *J. Comput. Chem*. **1999**, *20*, 730–748.

[46] Prime, version 3.0, Schrödinger, LLC, New York, NY, 2011.

[47] Kaminski, G. A.; Friesner, R. A.; Tirado-Rives, J.; Jorgensen, W. L. Evaluation and reparametrization of the OPLS-AA force field for proteins via comparison with accurate quantum chemical calculations on peptides *J. Phys. Chem. B* **2001**, *105*, 6474–6487.

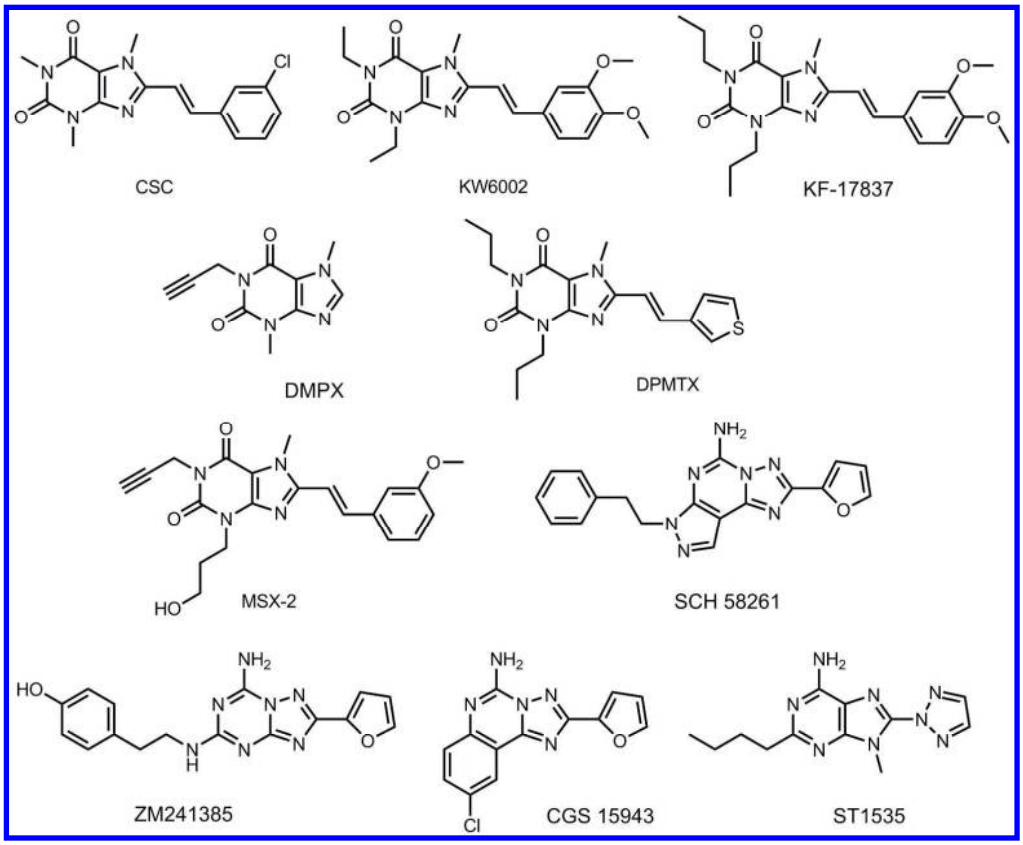

Figure 1. A2A receptor antagonists.
234x193mm (300 x 300 DPI)

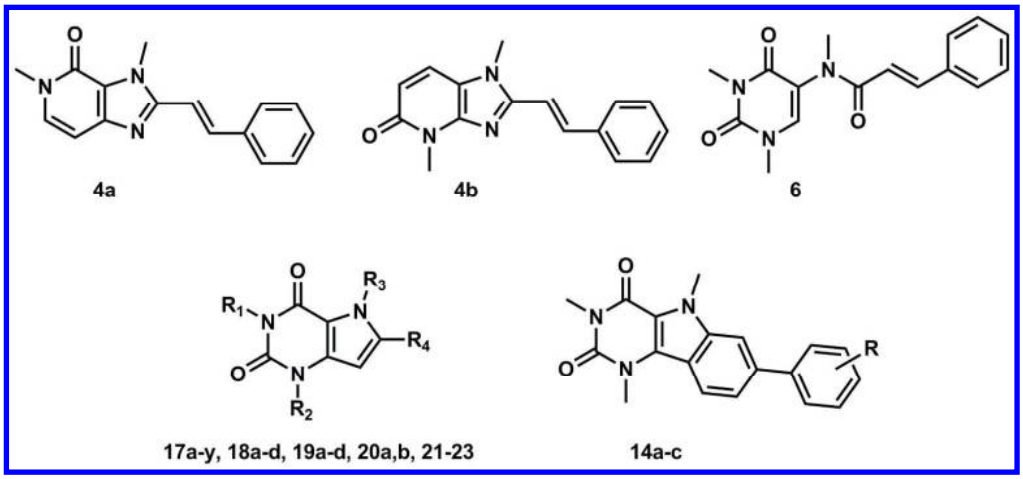

Figure 2. Chemical scaffolds of newly synthesized compounds.
204x93mm (300 x 300 DPI)

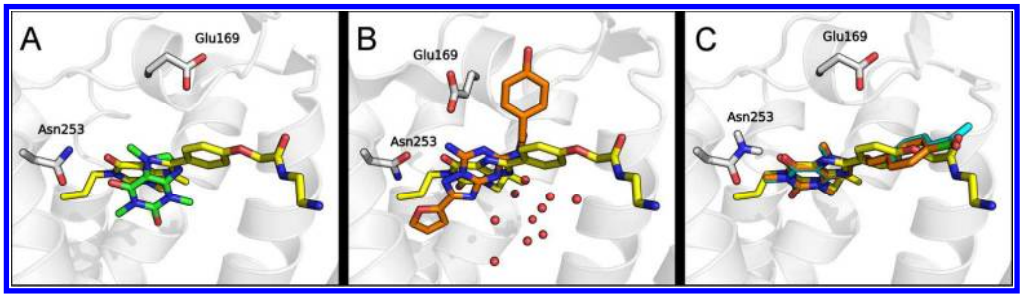

Figure 3. (A) Superposition of the crystal structures of A2A receptor in complex with caffeine (green carbons, PDB code: 3RFM) and XAC (yellow carbons, PDB code: 3REY). (B) Superposition of the crystal structures of A2A receptor in complex with ZM241385 (orange carbons, PDB code: 4EIY) and XAC (yellow carbons). Water molecules are represented with red spheres. (C) Best docking poses for compounds 17f (orange carbons) and 17q (cyan carbons) within the A2A receptor structure built from 3REY. XAC molecule is depicted with yellow carbons.
177x48mm (300 x 300 DPI)

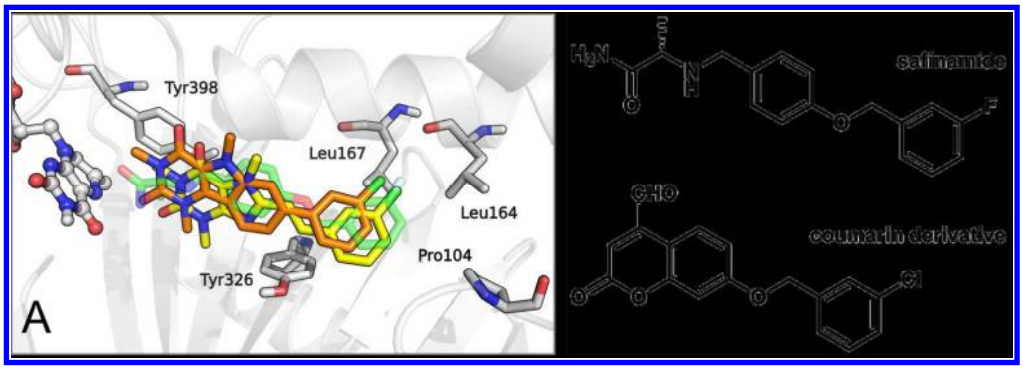

Figure 4. (A) Best docking poses for CSC (yellow carbons) and 14b (orange carbons) within the MAO-B active site. The co-crystallized safinamide is depicted with green transparent carbons and the FAD cofactor in ball-and-sticks with white carbons. (B) Chemical structures of MAO-B inhibitors safinamide and coumarin derivative.
177x61mm (300 x 300 DPI)

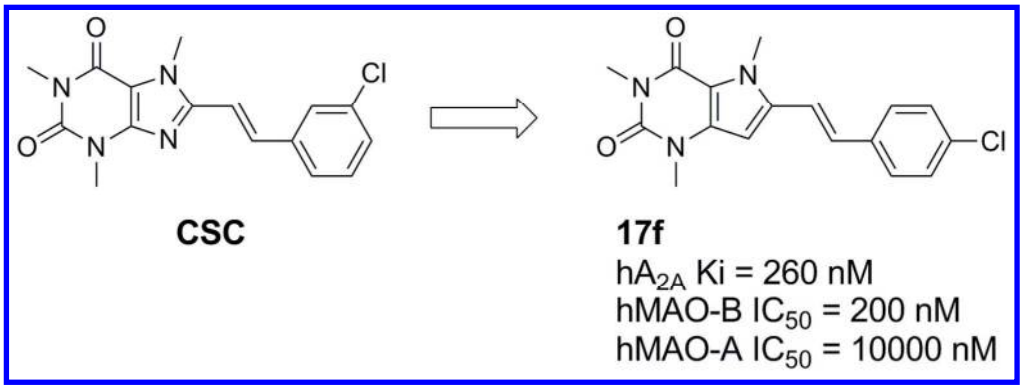

Table of Contents Graphic
127x46mm (300 x 300 DPI)